Reviews

Labile supramolecular structures and their dynamics in associated liquids based on NMR data

G. V. Lagodzinskaya, N. G. Yunda, and G. B. Manelis*

Institute of Problems of Chemical Physics, Russian Academy of Sciences, 1 prosp. Akad. Semenova, 142432 Chernogolovka, Moscow Region, Russian Federation. Fax: +7 (496) 514 3244. E-mail: lago@icp.ac.ru

The results of experimental research into structuration of associated pure liquids and electrolyte solutions in these liquids by NMR spectroscopy are summarized. The influence of self-organization on the rate and relay mechanism of proton mobility, chemical kinetics, and thermodynamics is analyzed.

Key words: associated liquids, hydrazines, mineral acids, electrolyte solutions, compositions and structures of labile supramolecular systems, kinetics and mechanism of proton exchange in liquids, disproportionation of perchloric acid, NMR spectroscopy.

1. Introduction

It is generally known that the medium effects play a considerable and, in many cases, decisive role in chemical processes. Hence, solvation and complexation in liquids have been extensively studied. This provided improved insight into these phenomena and progress in investigation of structural self-organization. At the same time, it should be noted that different experimental methods often give contradictory results, whereas theories generally deal with idealized simple liquids and infinitely dilute solutions. Many questions remain unclear for real systems (complex molecules, specific interactions, high concentrations, *etc*.). This is associated primarily with the importance of multiparticle correlations in liquids and the lack of adequate theories of the liquid state because of the difficulties in taking into account these correlations. Computer simulation methods for liquids, which have been extensively developed in recent years, hold considerable promise. However, these methods are far from being perfect because investigations are performed for a relatively small number of particles and are based on controversial assumptions. A versatile approach to the problem involving various experimental methods and computer simulation based on modern theoretical concepts is very promising for studying the specific features of liquids, effects of self-organization of its particles to form labile supramolecular structures, and their influence on chemical processes.

The chemical shifts, relaxation times, and line shapes in NMR spectroscopy are sensitive to intermolecular interactions although, like data from most other methods,

Published in Russian in *Izvestiya Akademii Nauk. Seriya Khimicheskaya,* No. 4, pp. 577—601, April, 2006.

1066-5285/06/5504-0597

give information averaged over different states. The vigorous development of NMR spectroscopy in the last decades, on the one hand, and achievements in computer simulation of liquids, on the other hand, open new possibilities for studies of the liquid state by NMR methods. In some cases, information on the compositions and structures of labile supramolecular systems can be extracted from high-precision measurements of concentration and temperature dependences of NMR parameters, and direct data on the lifetimes of solvated protons in liquids can be obtained from the kinetics of proton exchange.

The present review summarizes the results of our investigations on the effects of structuration in associated pure liquids, such as water, hydrazines, and mineral acids, and electrolyte solutions in these liquids by NMR spectroscopic methods. Examples of the decisive influence of self-organization on the rate and mechanism of proton exchanges, chemical kinetics, and thermodynamics are given.

2. H^+-Catalyzed symmetric proton exchanges in pure liquids and the supramolecular mechanism of relay proton mobility

In recent years, interest in the mechanism of proton migration in liquids, primarily, in water, has considerably quickened.[1—9] This is associated with both the abnormally high proton mobility and the importance of proton conductivity in various fields of science, such as materials science, physics, chemistry, and biology.[10] A direct comparison of the times of proton jumps from the proton conductivity and the times of molecular rotation from spin-lattice relaxation in D_2O showed[3] that the Stokes hydrodynamic contribution is insignificant and the relay (Grotthuss) mechanism plays the major role. This mechanism was fundamentally reviewed and detailed[2] and was modeled in different approaches.[1,4—6,8] It appeared that[8,9] the proton solvation complex in water taking into account the quantum effects is more likely a versatile fluctuating structural defect, whereas typical $H_9O_4^+$ and $H_5O_2^+$ are only the limiting "ideal" forms, which are present along with other species, though the latter being, apparently, less favorable. As a results of small (by fractions of an angstrom) migrations of "active" protons along strong hydrogen bonds (H bonds) in the center of the solvation complex, the cleavage of particular H bonds, and the formation of other H bonds at the periphery of the complex, the structure of the fluctuating solvation complex is transformed from one form into another and randomly migrates, thus transferring the excessive H^+ charge to the adjacent sites in the solvent lattice through the so-called "structural diffusion."

Analysis of experimental data on the rates and activation energies (E_a) of proton mobility and rotation motion of water molecules led to the conclusion[2] that the dynamics of H bonds in the second coordination sphere of H_3O^+ rather than rotation of water molecules in the vicinity of the solvation complex (as has been assumed earlier) is the rate-limiting step of Grotthuss mobility. This was confirmed by the results of computer simulation.[8]

It should be noted that the energy barriers of the processes under study are low, the accuracy of experimental data is insufficiently high, and calculations were carried out for a small number of molecules and included some assumptions. Hence, the progress achieved in understanding the molecular mechanism of the fundamental process of proton mobility in water need further verification and analysis. From this point of view, it is worthwhile to compare the proton mobilities in water with the data for other H-bonded liquids and reveal the general and individual features. In particular, it is interesting to elucidate the role of the structure pattern of liquids and the solvation H^+ complex in the migration of the H-bonded structure of the proton solvation complex in the H-bond network of the liquid. The most direct experimental data on the Grotthuss contribution to the proton mobility in liquids can be obtained by measuring the rates of proton exchange by NMR methods. The results of simulations should be compared with these experimental data.

Short settled proton lifetimes in the H^+ solvation complex (in water, $\sim 10^{-12}$ s) are difficult to measure by NMR spectroscopy. Under standard conditions, due to H^+-catalyzed fast proton exchanges, the average signal observed from the mobile protons of OH or NH groups of liquids is insensitive to the process rate. However, experiments with low H^+ concentrations allow one to increase the settled proton lifetime in liquid molecules to an extent that proton exchanges fall in the range of the so-called intermediate rates suitable for measurements and analysis of NMR spectra. This necessitates laborious special methods of purification from impurities but makes it possible to simultaneously extract valuable information on the molecular reorientation times from the quadrupole relaxation times of adjacent nuclei be measuring spectra with exchanges slow on the NMR time scale. In addition, in the case of slow exchanges, it becomes possible to obtain information independently of each group for liquids containing several chemically nonequivalent OH or NH groups.

Our detailed studies[11—17] of the kinetics and the mechanism of H^+-catalyzed symmetric proton exchanges in liquid hydrazines, self-association, and solvation of H^+ in these liquids by NMR spectroscopy demonstrated[14,15] that structural diffusion is the rate-limiting step of exchanges. This diffusion represents random migration of the H-bonded structure of the proton solvation complex in the liquid structure due to the H-bond rearrangement, *i.e.*, the Grotthuss component of the proton mobility. We performed[18] a comparative analysis of our results and the data published in the literature, which were obtained

predominantly by NMR spectroscopy in studies of H^+-catalyzed symmetric proton exchanges in systems with N—H...N and O—H...O hydrogen bonds, the molecular reorientational motion, self-association, and proton solvation for a number of H-bonded pure liquids, such as hydrazine and its methyl-substituted derivatives (our results), ammonia, methanol, and water (published data). This allowed us to obtain new data on the molecular mechanisms of the Grotthuss proton migration in H-bonded systems and the characteristic features of the solvation dynamics in these systems and propose an explanation for the observed differences in the rates and anomalies in the Arrhenius plots.

In some cases, we specifically designed experimental methods used for hydrazines. These methods were described in detail in Refs 11—15. Fast proton exchanges, which are generally observed in these liquids due to acid-like impurities from the atmosphere (CO_2) and from the vessel walls, were slowed down by performing a thorough purification[11] so that they were virtually absent on the NMR time scale. Small controlled amounts of H^+ (from 10^{-5} to 10^{-8} mol L^{-1}) were then added to the samples under study. The exchange rates and the quadrupole relaxation times of ^{14}N nuclei were obtained from the analysis of the ^1H NMR line shapes, and the correlation times of rotational motion were calculated from the quadrupole relaxation times.[12,15] Self-association of hydrazines[16] and proton solvation in these liquids[14,15] were studied.

2.1. Kinetics of proton exchanges and molecular reorientation. According to the laws of chemical kinetics, the following equilibrium occurs in H^+-catalyzed symmetric proton exchanges in pure liquids:

$$(H^+)_{solv} + B^*_{ass} \underset{}{\overset{k}{\rightleftharpoons}} (H^+)^*_{solv} + B_{ass}, \qquad (1)$$

where $(H^+)_{solv}$ are the solvated protons catalyzing the exchange, B_{ass} are molecules of the H-bonded liquid, and k is the rate constant averaged over all varieties of proton solvation complexes and liquid self-associates, including monomers; the fact of the proton exchange is marked with an asterisk. Equations (2)—(4) are valid for the rate $d[B]/dt$ of the chemical reaction (1), the exchange rate per molecule B $1/\tau_B$, and the exchange rate per the proton solvation complex $1/\tau_{H^+}$. Using these equations, k and $1/\tau_{H^+}$ can be calculated from $1/\tau_B$, which are directly determined in experiments.

$$d[B]/dt = k[B][H^+] \qquad (2)$$

$$1/\tau_B = (d[B]/dt)/[B] = k[H^+] \qquad (3)$$

$$1/\tau_{H^+} = (d[B]/dt)/[H^+] = k[B] \qquad (4)$$

The exchange rate $1/\tau_{H^+}$ is the Grotthuss component of the proton mobility and it is equal to the rate of structural diffusion for reactions limited by structural diffusion.[14] Nowadays, the leading role of structural diffusion in reactions (1) is beyond doubt, because it was established[19—21] that the frequency of proton transfers in strong N—H...N and O—H...O bonds is ~10^{13} s^{-1}, which is higher than the experimental values of $1/\tau_{H^+}$ by two—four orders of magnitude. Therefore, the problem is reduced to the determination of the detailed molecular mechanism of structural diffusion by itself.

The kinetic data[18] for proton exchanges and molecular reorientational motion and the hydrogen-bond energies in self-associates for pure liquids, such as hydrazine, monomethylhydrazine (MH), symmetrical and nonsymmetrical dimethylhydrazines (sDMH and nDMH, respectively), ammonia, methanol, and water, are presented in Fig. 1 and Table 1. It can be seen that at temperatures above room temperature, the inverse lifetimes of an excess proton at a particular oxygen or nitrogen atom, $1/\tau_{H^+}$, in water, methanol, and sDMH (and also in MH after extrapolation to this temperature range) are similar to the inverse correlation times of reorientational motion of liquid molecules $1/\tau_{corr}$ (τ_{corr} is equivalent to τ_{rot} [3]). For water, $1/\tau_{H^+}$ (see Fig. 1, curve *7*) are even larger than $1/\tau_{corr}$ (curve *7′*). At high temperatures, $1/\tau_{H^+}$ in methanol is also larger than $1/\tau_{corr}$. It should be noted that $1/\tau_{H^+}$ for water, which were determined from proton exchanges,[30] agree well with the data for the inverse times of proton jumps, $1/\tau_p$ (curve *7a*), which were calculated from the proton conductivity,[3] taking into account than only the jumps accompanied by changes in the proton spin (*i.e.*, 1/2 of the total number of protons) are observed in NMR spectra.

The existence of two exchange modes in sDMH (above and below 50 °C) is of particular interest. At temperatures above 50 °C, $1/\tau_{H^+}$ are similar to $1/\tau_{corr}$ and the activation parameters are typical of diffusion-controlled processes. At 50 °C, the Arrhenius plot has an inflection point, and the exchange much more substantially slows down with decreasing temperature, which is accompanied by an increase in E_a from 6.7 to 39.3 kJ mol^{-1}, whereas A_0 increases from 10^{12} to 10^{17}, which indicates that the character of solvation dynamics becomes more complicated. Similar abnormal activation parameters were observed in MH and methanol (see Table 1) as well as in supercooled water[3] (see Fig. 1, curve *7a*).

For other liquids, *viz.*, for hydrazine, nDMH, and ammonia, the rates $1/\tau_{H^+}$ are lower than the corresponding rates $1/\tau_{corr}$ by two—three orders of magnitude. For ammonia, this fact is attributed to low A_0, E_a = 9.2 kJ mol^{-1} being similar to E_{rot} = 7.5 kJ mol^{-1}. For hydrazines, this is associated with the fact that the activation energies are substantially higher than the activation energies of molecular rotation (20.1 and 16.7 kJ mol^{-1}; *cf.* 11.3 and 13.4 kJ mol^{-1} for hydrazine and nDMH, respectively).

To understand which factors are responsible for the rates of Grotthuss proton mobility in different liquids,

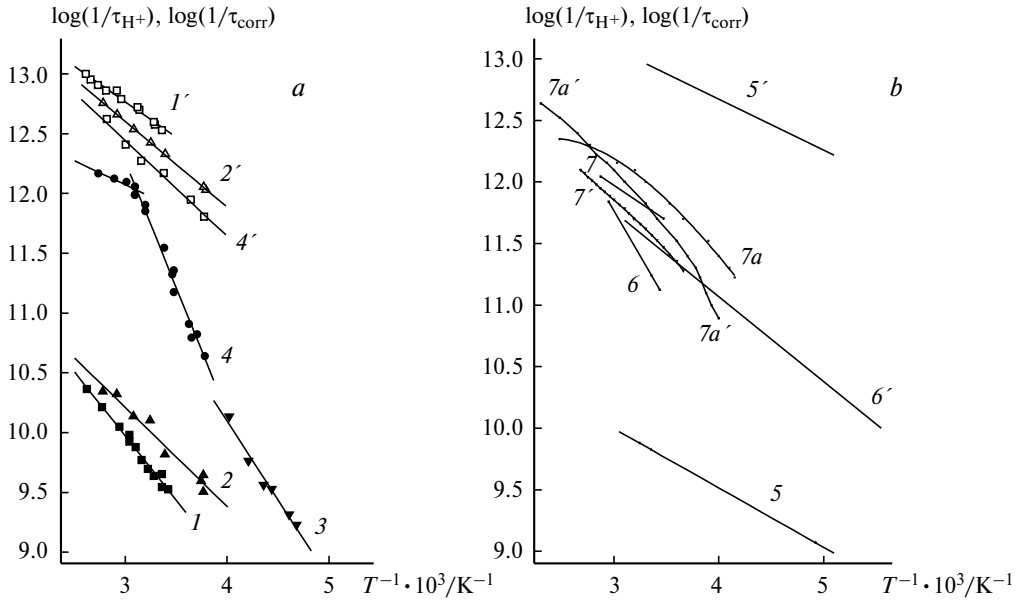

Fig. 1. Inverse lifetimes ($1/\tau_{H^+}$, *1*—*7*) of an excess proton (rates of proton migration) and inverse correlation times of molecular rotational motion ($1/\tau_{corr}$, *1′*, *2′*, *4′*—*7′*) in the Arrhenius coordinates determined in our studies for pure liquid N_2H_4 (*1*, *1′*), Me_2NNH_2 (*2*, *2′*), $MeHNNH_2$ (*3*), and MeHNNHMe (*4*, *4′*) (*a*) and published in the literature (*b*) for liquid ammonia (*5*, *5′*), methanol (*6*, *6′*), and water (*7*, *7a*, *7′*, *7a′*). The data for water (*7a*, *7a′*) were published in the study.[3] Other references and details are given in Table 1 and in the text.

Table 1. Parameters[a] of symmetric proton exchanges, quadrupole relaxation, and molecular reorientation in liquid B for the reaction (1)

Liquid B	k	A_0	E_a	E_{rot}	ΔE_{H_b}	$1/\tau_B$	$1/\tau_q$	τ_{H^+}	τ_{corr}
	L mol^{-1} s^{-1}		kJ mol^{-1}			s^{-1}		ps	
N_2H_4	$1.4 \cdot 10^8$ (see Refs 12, 17, 18)	$4.4 \cdot 10^{11}$ (see Refs 12, 17, 18)	20.1[12,17,18]	11.3[12,18]	—	14[12,18]	120[12,18]	220[15,17,18]	0.5[15,17,18]
Me_2NNH_2	$6.4 \cdot 10^8$ (see Refs 12, 17, 18)	$5.2 \cdot 10^{11}$ (see Refs 12, 17, 18)	16.7[12,17,18]	13.4[12,18]	10.0[16]	64[12,18]	200[12,18]	120[15,17,18]	0.7[15,17,18]
$MeHNNH_2$	$6.1 \cdot 10^9$ (see Refs 12, 17, 18)	$1.8 \cdot 10^{14}$ (see Refs 12, 17, 18)	25.5[12,17,18]	—	—	610[12,18]	—	8.7[15,17,18]	—
MeHNNHMe	$2.4 \cdot 10^{10}$ (see Refs 12, 17, 18)	$1.7 \cdot 10^{17}$ [b] (see Refs 12, 17, 18)	39.3[b,12,17,18]	15.5[18]	8.4[16]	2400[12,18]	343[18]	3.0[15,17,18]	0.9[15,17,18]
		$9.6 \cdot 10^{11}$ [c] (see Refs 17, 18)	6.7[c,17,18]						
NH_3	$1.2 \cdot 10^8$ (see Ref. 22)	$4.8 \cdot 10^9$ (see Ref. 22)	9.2[22]	7.5[23,24]	12.1[25]	12[22]	31[23]	150[22]	0.1[23]
MeOH	$2.7 \cdot 10^9$ (see Ref. 26)	$2.8 \cdot 10^{14}$ (see Ref. 26)	28.0[26]	13.2[27]	20.1[28]	120[26]	—	5.7[26]	1.1[29]
H_2O	$1.1 \cdot 10^{10}$ (see Ref. 30)	$9.4 \cdot 10^{11}$ (see Ref. 30)	10.9[30]	20.9[d] 14.6[e]	19.6[28]	1100[30]	—	1.7[30]	2.7[29]

[a] The rate constants k, the proton exchange rates $1/\tau_B$, the average lifetimes of an excess proton between two jumps during structural diffusion τ_{H^+}, the correlation times of molecular reorientation τ_{corr}, and the average quadrupole relaxation rates of $1/\tau_q$ are given for $T = 25$ °C. The proton exchange rates $1/\tau_B = k[H^+]$ are given for $[H^+] = 10^{-7}$ mol L^{-1}.
[b] $T < 50$ °C.
[c] $T > 50$ °C.
[d] At $T = 0$ °C.[29]
[e] At $T = 40$—100 °C.[29]

let us consider the data on the H-bonded structures of these liquids and proton solvation complexes in these liquids.

2.2. Self-association in pure liquids. The self-association is generally studied in dilute solutions in inert solvents. Unfortunately, contradictory experimental data on the H-bond topology and energy in pure liquids were obtained by different methods. According to the modern concepts, the percentage of nonbonded states in liquid water at room temperature is ~10%, and this percentage increases to ~20% at 100 °C. In the latter case, the loose structure of ice, although becoming fragmentary and imperfect, is to a large extent retained.[28,31] According to estimates obtained by different methods, the H-bond energy ΔE_{H_b} in water varies over a wide range (from 10.9 to 21.8 kJ mol^{-1}),[3] but this energy is generally assumed[31] to be approximately 20.9 kJ mol^{-1}. Methanol is also a strongly associated liquid containing long zigzag H-bond chains with rare branchings Y (OH groups, which are not involved in H bonds, account for several percentage).[28,32] It is assumed that ΔE_{H_b} for methanol is slightly higher than that for water.[28] Liquid ammonia is weaker associated, and there is no generally recognized models of its self-associates, although many models were proposed. According to recent data,[33] liquid ammonia consists of centrosymmetric heptamers analogous to fragments of the crystal structure. The energy difference ΔE_{H_b} determined as the photodissociation energy of clusters, in which the number of particles varies from four to eight, is 12.1 kJ mol^{-1}.[25] Based on the crystal structure, it is assumed that liquid hydrazine contains chain associates,[34,35] in which the H-bond energy is lower than that in water.[36] We demonstrated[16] that self-associates of nDMH and sDMH in inert solvents are cyclic trimers, in which the H-bond energy is 10.0 and 8.4 kJ mol^{-1}, respectively. Presumably, chain associates are also the major structures in these pure liquids.

Certain qualitative structural characteristics of the liquids in question can be obtained from the analysis of their chemical shifts in NMR spectra. Figure 2 shows the temperature dependences of the differences in the chemical shifts in the spectra of pure liquids and monomers, which can be approximately assumed to be equal to the chemical shifts from H bonds. The data for hydrazines were reported in our study.[18] The data for ammonia,[37] methanol,*,[38] and water[39] were published in the literature. The following values were used as the chemical shifts of the monomers (ppm relative to Me_4Si): hydrazine, 2.75 (directly measured in the gas phase in our study); nDMH, 2.74; sDMH, 2.48 (both values determined for the maximum dilution in CCl_4);[16] methylhydrazine, 2.48 for NH groups and 2.74 for NH_2;[16] ammonia, 0.23;[37] methanol, 0.898;[37,38] and water, 0.839.[39] It can be seen that the liquids under consideration can be divided into the following two groups: water and methanol, which have rather strong O—H...O bonds, $\Delta\delta_{H_b} \approx 4$—5 ppm, and all other solvents, *i.e.*, all hydrazines and ammonia, which form a tight group with $\Delta\delta_{H_b} \approx 0.5$—1.5 ppm and have rather weak N—H...N bonds. This classification is generally accepted in the discussion of H bonds in liquids. However, the facts that the proton chemical shifts for the H bonds are averaged over all protons and all molecular states and indirectly characterize the energy and the degree of the involvement of the molecule in the H-bond network of the liquid are not taken into consideration. Hence, the temperature dependence of the total chemical shift from H bonds per molecule ($\Delta\delta_{\Sigma H_b}$), which is determined by multiplying $\Delta\delta_{H_b}$ from the previous plot by the corresponding n (number of the NH or OH protons in the molecule involved in the exchange process)

$$\Delta\delta_{\Sigma H_b} = n\Delta\delta_{H_b} \quad (5)$$

are given in Fig. 3.

As can be seen from Fig. 3, the water molecule containing two OH groups is linked to the medium by H bonds two times stronger than the methanol molecule containing one OH group. Hydrazine, which forms rather weak

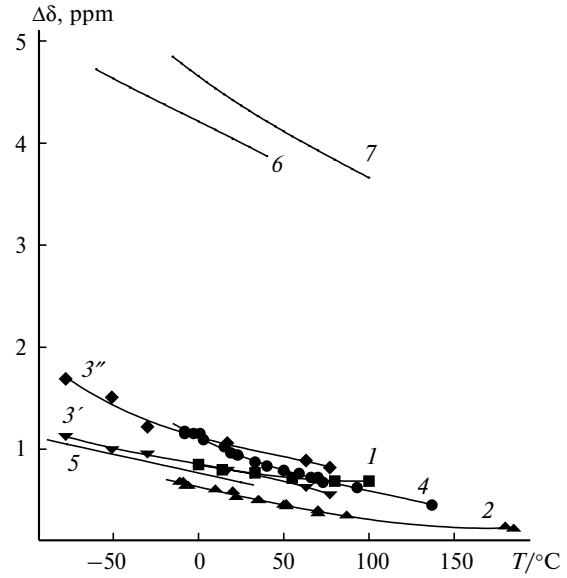

Fig. 2. Difference in the proton chemical shifts (Δδ) of the N—H or O—H groups in a pure liquid and in the corresponding monomer as the function of temperature for N_2H_4 (*1*), Me_2NNH_2 (*2*), $MeHNNH_2$ (NH, *3a′*; NH_2, *3″*), MeHNNHMe (*4*), NH_3 (*5*), MeOH (*6*), and H_2O (*7*).

* The internal chemical shift for the OH groups of the methanol molecule relative to the Me group of methanol as a function of the temperature was determined from the calibration plot of a methanol sample used as the temperature standard in Varian NMR spectrometers. For the chemical shifts of the Me groups relative to Me_4Si, δ is 3.34 ppm. The corrections for the magnetic susceptibility were applied according to a procedure described in the monograph.[37]

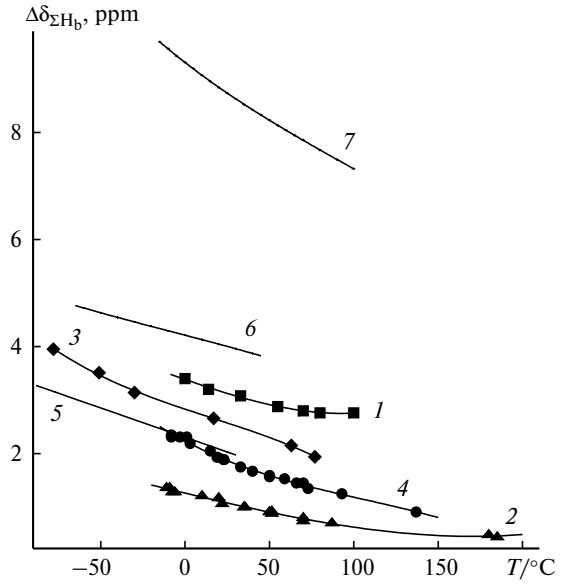

Fig. 3. Total proton chemical shift from the H bonds of the molecule $\Delta\delta_{\Sigma H_b} = n\Delta\delta_{H_b}$ for the N—H and O—H groups as the function of temperature T (n is the number of protons of the N—H or O—H groups in the liquid molecule). The numbering of the curves is identical to that in Fig. 2 (curve *3* corresponds to the sum of the data for the NH and NH_2 groups in $MeHNNH_2$).

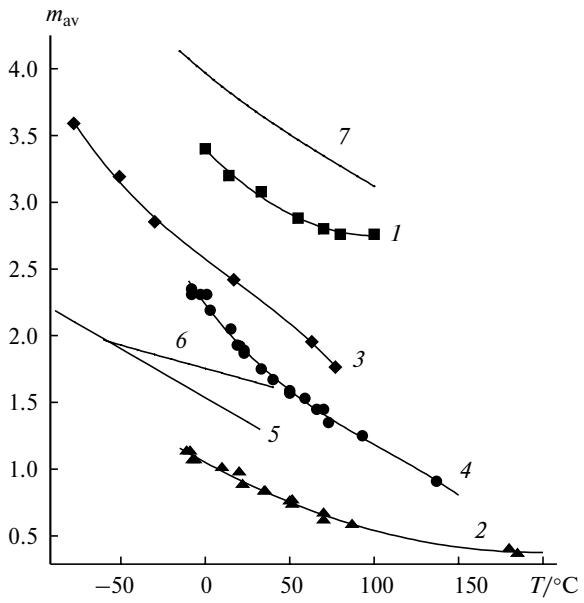

Fig. 4. Average number of H bonds formed by the molecule (m_{av}) in pure liquids as the function of temperature. The numbering of the curves is identical to that in Fig. 2 (curve *3* corresponds to the sum of the data for the NH and NH_2 groups in $MeHNNH_2$).

H bonds involving four NH groups, is similar to methanol. These liquids are followed by MH and NH_3. In terms of these concepts, the H bonds in the nDMH molecule make the smallest contribution.

The empirical relation between the chemical shifts from the H bond $\Delta\delta_{H_b}$ (in ppm) and the corresponding enthalpy of the H bond $-\Delta H_{H_b}$ (in kJ mol^{-1}) takes the following form:[40]

$$-\Delta H_{H_b} = 4.64\Delta\delta^0{}_{H_b} + 2.05, \quad (6)$$

where $-\Delta H_{H_b}$ are equal to ΔE_{H_b} (see Table 1),* $\Delta\delta^0{}_{H_b} = \Delta\delta_{\Sigma H_b}/m_{av}$ (m_{av} is the average number of H bonds formed by one molecule with the medium, which characterizes the H-bonded structure of liquids). From this it follows that

$$m_{av} = 4.64\Delta\delta_{\Sigma H_b}/(\Delta E_{H_b} - 2.05). \quad (7)$$

The plot of these parameters *vs*. the temperature is given in Fig. 4. In spite of the approximate character (due to the assumptions made), this plot is, on the whole, consistent with the published data obtained by other methods and clearly illustrates the H-bond network and its changes with temperature for all the liquids under consideration, including hydrazines, for which direct experimental data are lacking. For example, if the average number of H bonds per molecule $m_{av} \leq 2$ both for methanol and nDMH, as well as for sDMH, at temperatures above 50 °C, self-associates will be predominantly linear or cyclic with possible rare branchings; at $m_{av} > 2$, three-dimensional frameworks appear (water, $m_{av} \approx 3$—4; hydrazine, $m_{av} \approx 2.7$—3.3; MH, $m_{av} \approx 1.7$—3.5; sDMH at low temperatures, $m_{av} \approx 2.2$). Due to the uncertainty of the model of self-associates, it is difficult to draw conclusions about ammonia.

However, it should be noted that the framework in water differs substantially from that in hydrazines. In water, four vacancies of one molecule for the formation of H bonds (two donor and two acceptor vacancies) originate from one center, resulting in the known loose structure. In hydrazines, vacancies are distributed between two centers, and each center can be involved in different chain associates, which complicates the steric requirements for H bonding.

2.3. Proton solvation. Let us consider the data on the compositions and structures of proton solvation complexes in liquids. As mentioned in the Introduction, the aqueous solvation complex has been studied in most detail. Recently,[41] two types of linear and cyclic structural isomers have been found in studies of protonated methanol clusters. In these isomers, like in water, the proton is either located on one liquid molecule (cyclic complex $BH^+ \cdot 3B$ and the linear complex $BH^+ \cdot 4B$) or delocalized between two liquid molecules (linear complex $H^+ \cdot 4B$ and the cyclic complex $H^+ \cdot 5B$). It is reasonable to assume that the proton solvation complexes in liquid methanol have the same structures. Linear structures would be expected

* For hydrazine and MH, ΔE_{H_b} were taken equal to the corresponding values for nDMH and sDMH.

to be more favorable in liquids, because such structures are more readily involved in the structure of liquids. The "magic numbers" indicate that cluster ions containing the NH_4^+ cation in the center are the major structures for ammonia in the gas phase.[42] For liquid ammonia, information on the prevailing model of the proton solvation complex is lacking.

We obtained data on proton solvation in hydrazines using a method based on the detailed analysis of comprehensive high-precision measurements of the concentration dependences of chemical shifts[14,15] (this method is described below; see Section 3). To check the correctness of this method, the latter was also applied to aqueous solutions.[14,43]

The method consists in the following. For the dependences of the averaged chemical shifts on the composition for the B—HA systems (B is a base and HA is an acid), in which the A^- anion is weakly solvated by H bonds compared to the proton, the plots of δ *vs.* q (q is the generalized Gutovskii coordinate,[14] *i.e.*, the proportion of the protons of the acid of all the protons involved in the exchange) are nonsmooth linear-bent curves. Singular inflection points, *i.e.*, small but rather sharp changes in the slopes in the narrow concentration ranges, correspond to thermodynamically stable diffusion-averaged "ideal" structures of solvation H^+ complexes. Linear regions between two inflection points correspond to the dynamic equilibrium between these two solvation forms. The "magic numbers" of the molar concentration ratios [B] : [HA] at the inflection points are determined by the model of the solvation complex and correspond to the completed solvation structures with filled vacancies for H bonding in two coordination spheres in H^+- and/or BH^+-centered solvation complexes. In the concentration range, where the number of molecules B is too small to occupy two solvation spheres, models of solvation complexes, which impose weaker requirements upon the number of solvating molecules (with the inclusion in the coordination spheres of the anions, with the filling of only the first coordination sphere, *etc.*).

For the H_2O—$HClO_4$ system, the first inflection point at room temperature corresponds to the higher solvation complex $H_{27}O_{13}^+$ in which the first and second coordination spheres about the H_3O^+ ion are completely occupied.[14,43] This is evidence that, under the above-mentioned conditions, H_3O^+-centered structures are more favorable, although the situation is more complicated at higher temperatures and concentrations, and there is evidence that $H_5O_2^+$-centered structures become dominant.[43] These results are consistent with the modern concepts presented in the beginning of this section.

For hydrazine systems containing H_2SO_4 and HCl as HA, the inflection points correspond to the higher solvation complexes $H^+ \cdot 6B$ for both hydrazine and nDMH. For sDMH, the higher solvation complex has the composition $H^+ \cdot 4B$ according to the number of vacancies for H bonding in two coordination spheres in the H^+-centered models. Under the experimental conditions (20—100 °C for hydrazine, 64 °C for nDMH, and 74 °C for sDMH), no inflection points corresponding to BH^+-centered models of solvation complexes were found.[14,15]

2.4. Grotthuss (relay) proton migration. Taking into account the above-considered data on the structures of H-bonded liquids and proton solvation complexes and based on the recent concepts developed for water, let us consider the probable molecular mechanism of Grotthuss proton migration in liquids.

Based on the concepts for water, it can be suggested that the Grotthuss proton migration in all the liquids under consideration (see Fig. 1, Table 1) occurs through interconversions of the solvation structures, in which the proton is localized at one molecule B and delocalized between two molecules B:

$$(BH^+)_{solv} + B_{ass} \rightleftharpoons (BH^+B)_{solv} + B_{ass}. \qquad (8)$$

This process can be fast, *i.e.*, $1/\tau_{H^+} \approx 1/\tau_{corr}$, only if the energy difference between these solvation complexes is small. For water, this difference was estimated[7] at 2.5 kJ mol^{-1}, the H_3O^+-centered solvation complex being the prevailing structure at room temperature. This is consistent with our data.[14,43] In the case of a larger energy difference, the less favorable solvation complex would be expected to serve as a transition state, whereas the more favorable complex will serve as a proton trap.[7,8] In spite of the complexity of the structural motifs of water and proton solvation complexes in water, simulations demonstrated[8] that the H-bond network is easily rearranged. This is, apparently, favored by the small size of the molecule, the absence of inactive regions at its surface, and the equal numbers of the donor and acceptor centers.

In the series of the liquids under consideration, the high Grotthuss proton mobility is observed (in addition to water) in methanol and sDMH at temperatures above room temperature (see Fig. 1). It can be concluded that the energy difference between the solvation complexes $(BH^+)_{solv}$ and $(BH^+B)_{solv}$ in these liquids is small. Both liquids are characterized by similar one-dimensional chain structures of H bond motifs in both the self-associate and the proton solvation complex, which should facilitate isomerization (8), because the attachment—detachment of one molecule B is sufficient for this process.[15,17,18]

However, it should be taken into account that methanol is strongly associated, whereas sDMH is weakly associated (see Figs 3 and 4 and the text above). The activation parameters of proton exchange (both E_a and A_0, see Table 1) and, consequently, Grotthuss proton mobilities in these liquids at temperatures below 50 °C have similar abnormally high values, *i.e.*, the proton mobility is retarded with decreasing temperature much more sharply

compared to water. In weakly associated sDMH at temperatures above 50 °C, where m_{av} is smaller than 1.5 (*i.e.*, where the percentage of H-bonded states is smaller than 30% taking into account that the maximum m_{av} is 4), the activation parameters of the proton exchange are similar to those typical of water. In this case, $1/\tau_{H^+}$ is even larger than those in water and methanol although $1/\tau_{H^+}$ remains smaller than $1/\tau_{corr}$ as opposed to these two liquids.* In strongly associated methanol, the activation parameters are abnormal throughout the temperature range under study up to the boiling point, even when $1/\tau_{H^+}$ becomes larger than $1/\tau_{corr}$, analogously to water.

In our opinion, the abnormally sharp retardation of structural diffusion in methanol and sDMH with decreasing temperature is associated with the fact that the active regions of molecules B become less accessible with increasing degree of association of the liquid. If the amount of monomers in liquids is small, reaction (7) occurs predominantly with the involvement of self-associates B_{ass}, in which ordering due to H bonds and hydrophobic interactions gives rise to hydrophilic and hydrophobic nanoregions. In addition, the proton solvation complex can be incorporated into such self-associates. This leads to diffusion restrictions, resulting in the abnormally high activation parameters. In sDMH at temperatures above 50 °C, these restrictions are apparently eliminated due to a decrease in the degree of association.

Let us consider another pair of liquids with similar behavior, *viz.*, hydrazine and nDMH, in which the exchange rate constants are two orders of magnitude lower than those in water. As can be seen from Figs 3 and 4, these liquids strongly differ in the degree of association. Of all the hydrazines under study, nDMH is the least associated liquid with rare chain associates, whereas hydrazine is, on the contrary, the most strongly associated liquid. Two nitrogen atoms of hydrazine are involved in different chain associates with high probability to form a three-dimensional H-bond network. At the same time, according to our data,[15] the prevailing proton solvation complexes in these liquids have the same composition and structure, *viz.*, {2B(BH^+B)2B}. The pre-exponential factor is approximately equal to the number of collisions in liquids (10^{11}),[44] and the activation energy is substantially higher than E_a in water, which is referred to the dynamics of H-bond cleavage in the second coordination sphere of the proton solvation complex. These activation parameters can correspond to isomerization (7) limited by the transition through the barrier. According to the concepts for water,[7,8] the energetically unfavorable form of the solvation complex can serve as the activated state. According to our data on the structures of proton solvation complexes, the solvation complexes $(BH^+B)_{solv}$ are favorable for all the hydrazines under study. Apparently, the energy difference between two types of the solvation complexes, *viz.*, $(BH^+B)_{solv}$ and $(BH^+)_{solv}$, in hydrazine and nDMH in the case of exchange between NH_2 is substantially larger than that in sDMH in the case of exchange between NH. Hence, the activation energy of proton exchanges becomes the measure of this difference.

The proton exchange rates in ammonia $1/\tau_{H^+}$ are approximately a hundred times lower than those in water and are approximately equal to the rates in hydrazine and nDMH, although the temperature dependences are sharply different. The activation energy in ammonia (9.2 kJ mol^{-1}) is close to E_a in water (and for the high-temperature region of sDMH), and retardation is completely due to a decrease in A_0 by two orders of magnitude (see Table 1). The low energy E_a indicates that the energy of the solvation complexes $(BH^+)_{solv}$ is close to that of $(BH^+B)_{solv}$. Apparently, the pre-exponential factor decreases due to the topological difficulties of the rearrangement of the H-bond network in proton solvation complexes and self-associates with complicated structures.[25,33,42] These difficulties can be partly attributed to the fact that the number of donor capabilities for the formation of H bonds differs from the number of acceptor capabilities, because there are three protons per lone electron pair in the ammonia molecule. In the case of isomerization (7), it is these deficient lone electron pairs that are necessary for the rearrangement of one form of the proton solvation complex into another form.

In the series of the liquids in question, MH stands out. For MH, the temperature dependence of $1/\tau_{H^+}$ (see Fig. 1) looks like an extrapolation of the data for sDMH to the low-temperature region. It seems that of three possible exchange reactions (NH with NH, NH_2 with NH_2, and NH with NH_2) in MH, one reaction is the major process. This is not surprising because the exchange between NH is approximately a hundred times faster than that between NH_2, whereas the exchange between NH and NH_2 does not, apparently, make a noticeable contribution due to the energy asymmetry. This is consistent with the fact that, although MH is more associated than sDMH (see Figs 2—4), this occurs due to the contribution of NH_2, whereas the contribution of NH is approximately the same in both liquids. Apparently, the symmetric H bonds between NH, like those between NH_2, are more favorable than asymmetric bonds between NH and NH_2 with the result that the nearest environment of each group is formed predominantly by the same groups, particularly, with decreasing temperature. Hence, the local structure in the vicinity of NH in MH is approximately identical to that in sDMH and, consequently, the temperature dependences of $1/\tau_{H^+}$ are also identical due to the identical diffusion hindrance.

* This fact can be attributed to the larger size and the more complex structure of the sDMH molecule (the presence of two reaction centers).

Table 2. Supramolecular mechanism of proton exchanges and Grotthuss proton migration $(BH^+)_{solv} \rightleftharpoons (BH^+B)_{solv}$ in liquids B

Liquid B	k	A_0	E_a	ΔH_{solv}*	Mechanism of H^+ mobility
	L mol^{-1} s^{-1}		kJ mol^{-1}		
N_2H_4	$1.4 \cdot 10^8$	$4.4 \cdot 10^{11}$	$20.1 \approx \Delta H_{solv}$	$>RT$	$(BH^+B)_{solv}$ is the proton trap,
Me_2NNH_2	$6.4 \cdot 10^8$	$5.2 \cdot 10^{11}$	$16.7 \approx \Delta H_{solv}$	$>RT$	$(BH^+)_{solv}$ is the transition state
$MeHNNH_2$	$6.1 \cdot 10^9$	$1.8 \cdot 10^{14}$	25.5	$<RT$	Structural diffusion of $(H^+)_{solv}$
MeHNNHMe ($T < 50$ °C)	$2.4 \cdot 10^{10}$	$1.7 \cdot 10^{17}$	39.3	$<RT$	hindered by nanoheterogeneity of the liquid
MeHNNHMe ($T > 50$ °C)	$1.0 \cdot 10^{11}$	$9.6 \cdot 10^{11}$	6.7	$<RT$	Structural diffusion of $(H^+)_{solv}$
NH_3	$1.2 \cdot 10^8$	$4.8 \cdot 10^9$	9.2	$<RT$	Structural diffusion of $(H^+)_{solv}$ slowed down by the complex topology of the structure of solvation complexes $(H^+)_{solv}$ and self-associates
MeOH	$2.7 \cdot 10^9$	$2.8 \cdot 10^{14}$	28.0	$<RT$	Structural diffusion of $(H^+)_{solv}$ hindered by nanoheterogeneity of the liquid
H_2O	$1.1 \cdot 10^{10}$	$9.4 \cdot 10^{11}$	10.9	$<RT$	Structural diffusion of $(H^+)_{solv}$

* ΔH_{solv} is the energy difference between solvation of $(BH^+)_{solv}$ and $(BH^+H)_{solv}$.

Therefore, a comparative analysis of our results and experimental data published in the literature on the kinetics of H^+-catalyzed symmetric proton exchanges, molecular reorientational motion, self-association, and proton solvation for a series of H-bonded pure liquids with N—H...N and O—H...O bonds taking into account the latest results of simulation of the Grotthuss proton mobility in water led to the revision, refinement, and generalization of the concepts on the molecular mechanism of these fundamental processes (Table 2). It can be concluded that, although exchanges (and Grotthuss mobility) in all systems with N—H...N and O—H...O bonds occur through interconversions of two type of solvation complexes, *viz.*, $(BH^+)_{solv}$ and $(BH^+H)_{solv}$, *i.e.*, through diffusion of the structural defect caused by an excess proton in the structure of the H-bonded liquid, this structural diffusion is the rate-determining step only in systems, where the energy difference between these solvation complexes is small (water, sDMH, or methanol); otherwise, the most favorable solvation complex serves as a proton trap, whereas the unfavorable complex acts as the transition state. In this case, the process slows down (hydrazine or nDMH). Structural diffusion can also slow down because of two factors: the topological difficulties due to the complexity of the structures of solvation complexes (like in ammonia) or (in the case of simple structures of solvation H^+ complexes present in methanol and sDMH) diffusion hindrance due to "nanoheterogeneity" of strongly associated liquids (formation of nanosized hydrophilic and hydrophobic regions). Data on the influence of the methyl substituents indicate that the Grotthuss contribution to the proton mobility in liquids can be controlled within a wide range.

3. Supramolecular structures in electrolyte solutions in H-bonded liquids

Detailed studies of electrolyte solutions in associated solvents by NMR spectroscopy performed by different authors demonstrated that some concentration and temperature dependences* of the chemical shifts and the relaxation rates $1/T_1$ and $1/T_2$ are described by nonsmooth linear-bend curves.[14,15,17,43,45–49] In some cases, the dependences were characterized[48] by sharp changes at special points not only of the derivatives of NMR parameters but also of $1/T_2$. There are data on the nonsmooth character of the concentration plots for other physicochemical properties, such as the conductivity,[50] the density,[43] and the heat of mixing.[48] At special points, the compositions are generally characterized by magic integer molar concentration ratios.

These effects have attracted interest because they are undoubtedly related to the structure of electrolyte solutions at high concentrations, for which the theory remains to be developed. However, these phenomena have not gained wide recognition because the physical basics of these phenomena remain unclear.

The occurrence of these effects and the possibility of their study by NMR methods were unambiguously confirmed by the following factors: 1) large number of experiments performed for different systems by different research groups; 2) our data obtained with the use of difference derivatives; 3) identity of the results in the test experiments using independent series of samples; 4) cor-

* For the correctness, the linearization coordinate q, *viz.*, the Gutovskii coordinate generalized for nonaqueous media (see Ref. 14), should be used as the concentration.

relation of the characteristic features of the concentration dependences of the NMR parameters with the data on the densities[43] and heats of mixing.[48]

In our opinion, certain thermodynamically stable diffusion-averaged solvation structures, which can be called "unit cells of the liquid" by analogy with the unit cells of crystals, correspond to the singular points in the concentration plots for various physicochemical properties (inflection points, bent points, and extremums). Presumably, in simple cases, these structures are completed and contain filled vacancies for H bonding in either two or only one (first) solvation shells about ions (in aqueous solutions of perchloric acid[43] and hydrazine solutions of hydrazonium salts[14,15]).

In the case of intermediate compositions, the system in linear regions of the curves between two inflection points is a quasi-ideal mixtures of two such structures existing in a dynamic equilibrium.[14,15,17,43,48] At inflection points, one of the structures disappears, a new structure is formed, and the equilibrium between one pair of structures is transformed into the equilibrium between another pair. In some cases, sharp changes not only in the derivatives but also in the physicochemical parameters are observed in the vicinity of the special points. These effects are most pronounced in the N_2O_5—HNO_3 system, where 100% nitric acid acts as the solvent and N_2O_5 serves as a strong electrolyte. The pronounced narrow extremums in the curve of the heats of mixing correspond to the special points in the concentration plots for the chemical shifts and $1/T_2$ in the ^{17}O NMR spectra.[48]

The available theories and computer models for electrolyte solutions satisfactorily describe only dilute solutions, the solvent being generally considered as a continuous structureless medium. Numerous experimental data obtained by different methods[51,52] primarily for aqueous systems do not rule out the existence of diffusion-averaged prevailing structures and dynamic equilibria between pairs. However, these data are insufficiently detailed and precise to find these structures.

The structures of concentrated electrolyte solutions in H-bonded systems in nonaqueous media were poorly studied.[51] However, we most clearly observed[15,48] these effects in such systems due, apparently, to the great role of the molecular aspects of solvation for solvents composed of nonspherical molecules larger than H_2O. Apparently, the modern theories of electrolytes are unsuitable for concentrated solutions because these theories do not adequately take into account the molecular aspects of solvation. Therefore, investigations of the fine features of the concentration and temperature dependences of various physicochemical properties, including the NMR parameters, should be helpful in developing adequate models.

Experimental studies of these effects are very laborious and, in the absence of the corresponding theoretical basics, cast doubt. At the same time, we successfully used the developed model concepts in studies of the proton mobility in liquids[18] and disproportionation of 100% $HClO_4$.[53] Undoubtedly, these concepts will be useful in other cases. A further progress in this very interesting (in our opinion) field would be achieved by performing comparative calculations of liquid structures in the vicinity of special points and for intermediate compositions by the molecular dynamics (MD) method.

The $HClO_4$—H_2O system with the prevailing $[(H_3O^+)\cdot 3H_2O]\cdot 9H_2O$ structure is the simplest system characterized by a well-defined special point for the 1 : 13 composition. We have studied this system in detail. According to our nomenclature, this is the higher proton solvation complex. Due to rather weak H bonds with water, the ClO_4^- anion is, apparently, incorporated into the cavities between these structures so that it has no influence on the proton chemical shift unlike, for example, the HNO_3—H_2O system, where the H bonds of the anion complicate the situation.

The procedure used for high-precision measurements and analysis of the results was documented in the studies;[43,48,49] the data published in the studies[39,54—59] were also used.

3.1. Aqueous-acid $HClO_4$—H_2O, HNO_3—H_2O, and HCl—H_2O systems. The plots of the difference derivative $\Delta\delta/\Delta q$ in the $HClO_4$—H_2O system on the composition and temperature[43] are shown in Fig. 5, *a*. The corresponding plots $\delta(q)$ (Fig. 6) are consistent with the earlier data.[14,54] The curves for $\Delta\delta/\Delta q$ (see Fig. 5, *a*) are wave-like. Although the specific features observed as smoothed steps (see the inset to Fig. 5, *a*) are insignificant, they are several times larger than the measurement error and are reproduced in different series in certain concentration and temperature ranges. The steps are most clearly seen at 140 °C for the 1 : 4 and 1 : 3 compositions, which correspond to the crystal hydrates observed in the fusion diagram.[60] The observed inflection regions are extended by $\Delta q \approx 0.02$, which is larger than the smoothing of the steps achieved by taking the difference derivative (see the inset to Fig. 5), *i.e.*, the true inflection regions are $\Delta q \approx 0.01$. These steps are smeared out with decreasing temperature, whereas the specific features are rather clearly observed at 10, 24, and 70 °C at low concentrations for the 1 : 13 composition. We have observed this phenomenon earlier.[14] According to the principle of the construction of proton solvation complexes by filling the vacancies for H bonds,[14,15] this composition corresponds to hydrate $H_{27}O_{13}^+$ in which the first and second coordination spheres about the H_3O^+ ion are completely filled.

The seeming inflection region $\Delta q \approx 0.01$ is similar to the smearing region due to the procedure used for taking the difference derivative. Consequently, the true inflection region is small.

It should be noted that at 70 and 100 °C, the step appears also in the case of the composition approximately

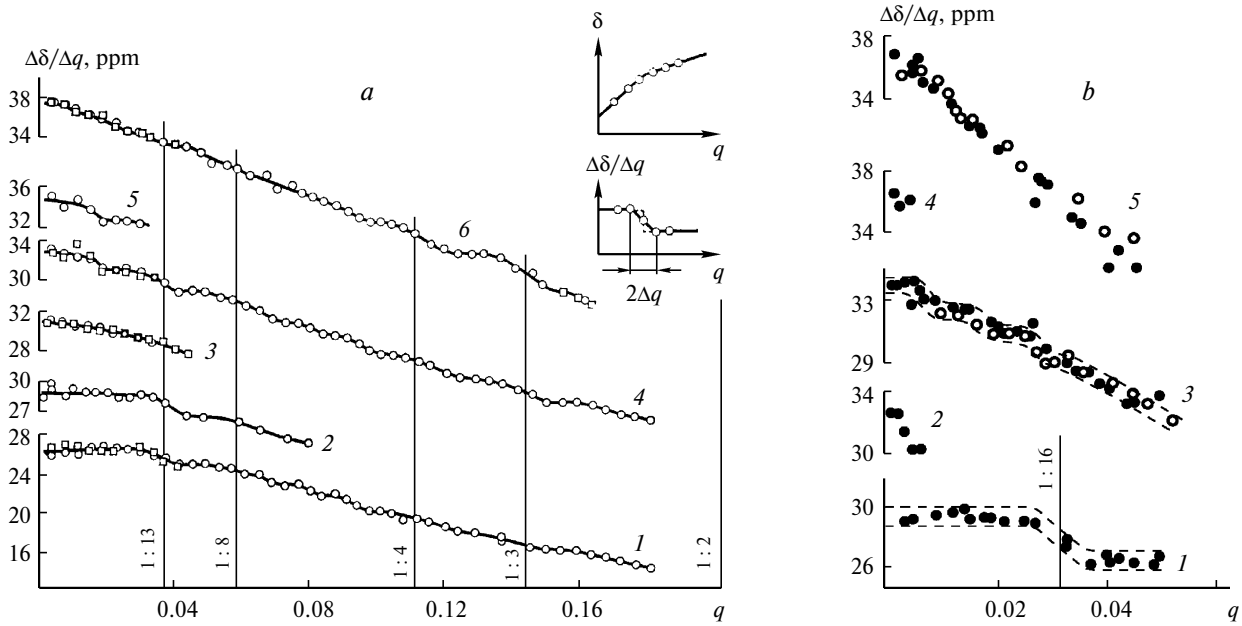

Fig. 5. Composition and temperature dependences of the difference derivative of the proton chemical shifts of aqueous-acid systems with respect to the linearization coordinate q (hereinafter, $q = x/(2 - x)$, where x is the molar fraction of the acid): *a*, the $HClO_4$—H_2O system at 10 (*1*), 24 (*2*), 45 (*3*), 70 (*4*), 100 (*5*), and 140 °C (*6*); the inset schematically illustrates the smearing effect for the inflection region due to the procedure used for taking the difference derivative; *b*, the HNO_3—H_2O system at 1 (*1*), 10 (*2*), 25 (*3*), 47.5 (*4*), and 70 °C (*5*).

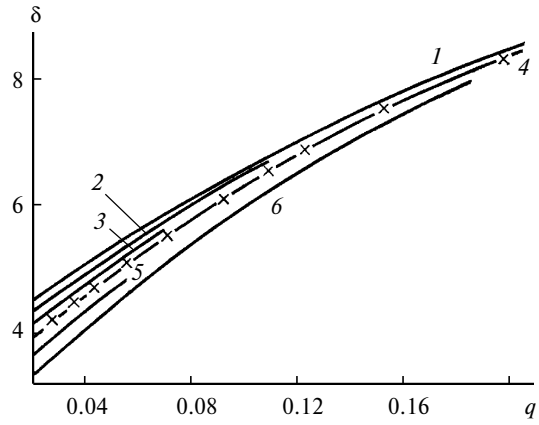

Fig. 6. Dependence of the proton chemical shifts in the $HClO_4$—H_2O system on the composition at 10 (*1*), 24 (*2*), 45 (*3*), 70 (*4*), 100 (*5*), and 140 °C (*6*); the results of the study[54] obtained at 65 °C are marked with a cross; the chemical shifts were converted relative to gaseous H_2O based on the data of the study.[54]

equal to 1 : 30, which corresponds to a hydrate more enriched in water. This is, apparently, due to changes in the H-bonded structure of water and is consistent with the concepts that the degree of hydration increases with increasing temperature.[61] Apparently, a step with the extended inflection region is observed at 10, 24, and 70 °C for the 1 : 8 composition corresponding to the proton hydrate $H_{17}O_8^+$ containing $H_5O_2^+$ at the center and the filled next solvation shell, $(H_5O_2^+)\cdot 6H_2O$. Presumably, there are specific features also in the regions of the compositions from 1 : 8 to 1 : 4, but these features cannot be detected by the available methods.

Therefore, the available data show that the chemical shifts depend in a complex way on the composition and temperature due to the complexity of structural rearrangements in the system. From the linear-bent character of $\delta(q)$ it follows[14,15,43,54] that within each linear region, the $HClO_4$—H_2O system is a mixture of two thermodynamically stable structural forms existing in the dynamic equilibrium, and the chemical shifts of these forms are independent of the composition. In dilute solutions, these are water and a higher hydrate, then a higher hydrate and hydrate containing a smaller amount of water, *etc*. It should be noted that not all possible compositions of solvation structures exist in solution with equal probability. As in the case of proton solvation in hydrazines,[14,15] the solvation complexes with the filled vacancies for H bonding in the coordination spheres are favorable up to rather high concentrations. Based on the compositions of the hydrates, it can be concluded that both H_3O^+- (1 : 13) and $H_5O_2^+$-centered (1 : 8) hydrates exist in the $HClO_4$—H_2O system depending on the conditions, which agrees with the small energy difference between these forms,[8,9] although this is inconsistent with the data[62] on the absence of H_3O^+-centered hydrates in aqueous acids. The fact that completed structures are more favorable than "incomplete" structures is, apparently, attributed to

the geometric factors (close packing requirements). These hydrates, being similar to the elements of the water structure, are better incorporated into water. In concentrated solutions, the number of hydrated structures increases.

From the fact that the chemical shifts of hydrates are independent of the composition it follows that these hydrates are included in the water structure in such a way that they virtually do not disturb its H bonds, and the H bonds between the peripheral hydrate molecules are equivalent to the H bonds in pure water. Solutions whose compositions are close to the inflection points consist predominantly of one structure, and smearing of the inflection region in $d\delta/dq$ characterizes the presence of impurities of other structures.

Analysis of the temperature dependence of the chemical shifts in the system under study confirms these concepts. A decrease in the temperature coefficients of the chemical shifts with increasing concentration of the acid (Fig. 7) is associated with an increase in the percentage of strong H bonds in the system. It is known that a decrease in the chemical shift of the average signal for the protons in H-bonded systems is primarily attributed to the H-bond cleavage due to thermal motion. If the H-bond energy is high compared to kT, the percentage of the cleaved H bonds is insignificant, and the chemical shift weakly depends on the temperature. Hence, it can be concluded that the temperature coefficient is associated with relatively weak H bonds between the proton hydrates in the concentration region $q > 0.04$, where free water is virtually absent in the system. The good agreement with the observed values can be achieved (see Fig. 7) on the assumption that the temperature coefficient for the chemical shifts of the peripheral protons in hydrates is equal to that in neat water, and the chemical shifts of the internal protons involved in strong H bonds are temperature independent and by estimating $d\delta/dT$ for hydrates based on their structures (taking into account the proportion of the peripheral protons, *i.e.*, the protons making a contribution to the temperature coefficient, of all the protons of the hydrate, and the ratio of protons to lone electron pairs in the outer coordination sphere of the hydrate, which determines the proportion of the peripheral protons capable of being involved in weak H bonds). For example, the chemical shift estimated for hydrate $H_9O_4^+$ ($q = 0.111$), which contains six peripheral protons and three lone electron pairs in the outer coordination sphere, is $(6/9)\cdot(3/6)(-1\cdot10^{-2}$ ppm deg$^{-1}) = -3.3\cdot10^{-3}$ ppm deg^{-1}, which is virtually equal to the observed value ($-3.2\cdot10^{-3}$ ppm deg^{-1}). For hydrate $H_{17}O_8^+$ ($q = 0.059$) containing seven internal and ten peripheral protons per eight lone electron pairs in the outer sphere, the expected value of $d\delta/dT$ is $(10/17)\cdot(8/10)(-1\cdot10^{-2}$ ppm deg$^{-1}) = -4.7\cdot10^{-3}$ ppm deg^{-1}, whereas the observed value is $-5.3\cdot10^{-3}$ ppm deg^{-1}.* Within the framework of these assumptions, it follows that the proton hydrates are actually linked to each other by H bonds, whose characteristics are similar to those in neat water. Apparently, this is possible due to the fact that, although the H-bond lengths in hydrates change, the tetrahedral coordination typical of water is retained (Fig. 8).

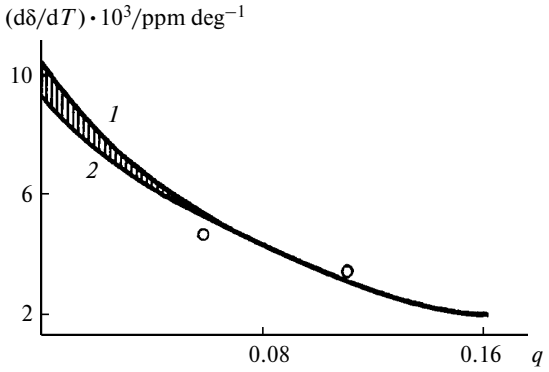

Fig. 7. Dependence of the temperature coefficient of the chemical shifts for aqueous solutions of perchloric acid on the composition at 10 (*1*) and 140 °C (*2*); the calculated values are represented by open circles (see the text).

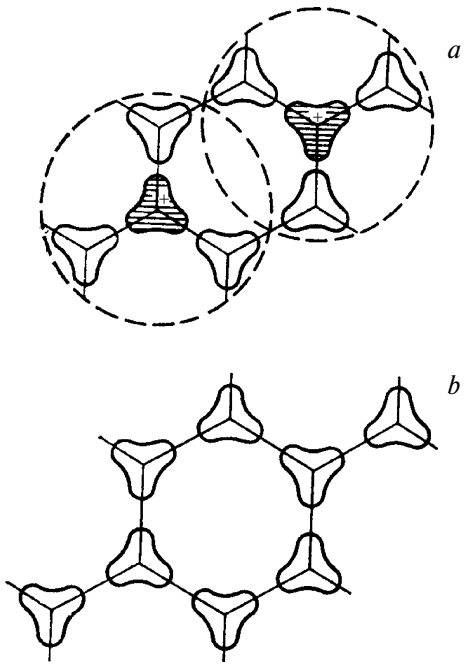

Fig. 8. Schematic representation of the structures of hydrate $H_9O_4^+$ (*a*) and water (*b*).

* For the 1 : 13 hydrate, this approach gives a strongly underestimated value ($-4.5\cdot10^{-3}$ ppm deg^{-1} instead of the experimental value of $-6.5\cdot10^{-3}$ ppm deg^{-1}) because, apparently, the assumption that the chemical shifts are temperature independent is incorrect for H bonds between the first and second coordination spheres. The estimate ($-6.1\cdot10^{-3}$ ppm deg^{-1}) similar to the experimental data can be obtained with the use of the temperature coefficient for these bonds half as large as that for water.

Let us consider the temperature dependence of the derivative $d\delta/dq$ in dilute solutions with $q \to 0$. Within the first linear region,

$$\left.\frac{d\delta}{dq}\right|_{q\to 0} = \frac{d}{dq}[p_h\delta_h + (1 - p_h)\delta_{H_2O}],$$

where p_h is the proportion of protons in the higher hydrate, and δ_h and δ_{H_2O} are the chemical shifts of the hydrate and water, respectively. Since $p_h = (2n + 1)q$, we have

$$\left.\frac{d\delta}{dq}\right|_{q\to 0} = \frac{d}{dq}\{(2n + 1)q\delta_h + [1 - (2n + 1)q]\delta_{H_2O}\}|_{q\to 0} =$$

$$= (2n + 1)(\delta_h - \delta_{H_2O}) = S_\Sigma,$$

where n is the number of water molecules in the higher hydrate and S_Σ is the total chemical shift of the higher hydrate relative to liquid water at the same temperature. An increase in S_Σ with increasing temperature (Fig. 9, curve *1*) reflects an increase in the hydration energy of the proton included in H bonds of the hydrate compared to the H-bond energy of the same number of water molecules in liquid water and is associated with the relatively larger degree of H-bond cleavage in water compared to the hydrate. Taking into account the almost linear dependence $d\delta/dT$ for water (deviations from the linearity for the temperature range under study is ~5%), the observed dependence $S_\Sigma(T)$ can be represented as two linear regions with an inflection point at ~30 °C, and the change in the slope of dS_Σ/dT can be attributed to the change in the composition (and in the structure) of the higher hydrate. This agrees well with the appearance of a step in the plot of $d\delta/dq$ for the ~1 : 30 composition at 70 and 100 °C, the absence of the step at 10 and 24 °C, and the intermediate character of the dependence of $d\delta/dq$ at 45 °C.

The changes in the solution structure observed in studies of the chemical shifts would be manifested in other physicochemical properties as well. However, it should be taken into account that different properties differ in the sensitivity to the changes in the solution structure, and it is necessary to have rather precise and detailed experimental data. Actually, the tendency of the system to undergo structural rearrangements is reflected in the fusion diagram[60] as numerous maxima corresponding to a series of crystal hydrates with compositions 1 : 1, 1 : 2, 1 : 2.5, 1 : 3, 1 : 3.5, 1 : 4, and 1 : 5.5 (see the inset to Fig. 10).

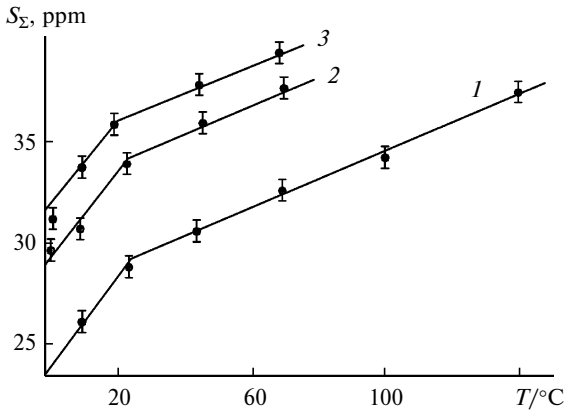

Fig. 9. Temperature dependence of the total chemical shift of higher hydrates (S_Σ) (see the text) for $HClO_4$ (*1*), HNO_3 (*2*), and HCl (*3*).

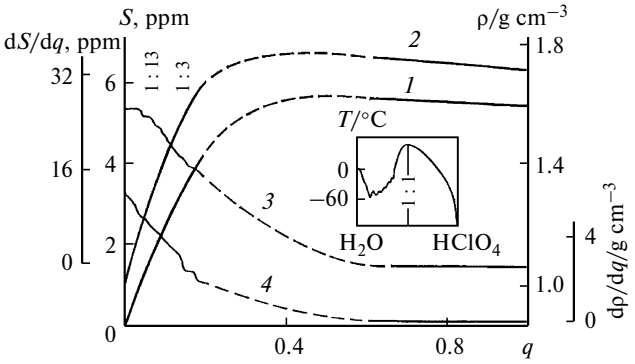

Fig. 10. Dependence of the proton chemical shifts relative to liquid water (S) at 10 °C (*1*), the density (ρ) at 25 °C (*2*), and the derivatives dS/dq (*3*) and $d\rho/dq$ (*4*) on the composition of the $HClO_4$—H_2O system according to the results of the studies.[43,54,60] The inset shows the fusion diagram.[60]

In addition, taking into account the above-described structural changes, the change in the proton chemical shift S* would be expected to correlate with the change in the density ρ of the system under study. This was confirmed by the data on the densities.[60] The values of $\rho(q)$ and $S(q)$ and the derivatives $d\rho/dq$ and dS/dq are presented in Fig. 10. Throughout the concentration range from $q = 0$ to $q = 1$, ρ changes in parallel with S (see Fig. 10). At the same time, it can be seen from the plots for the derivatives that both plots have a complex character, the special points not always being identical. For example, the proton chemical shifts are independent of the changes in the plot of $d\rho/dq$ for the compositions approximately equal to 1 : 3 and 1 : 2.5, which correspond to two of numerous crystal hydrates. These discrepancies at high concentrations are clear because, in addition to H bonds, electrostatic interactions between ions play a considerable role in the solution structure. At rather low concentrations, where H bonds play the decisive role, the specific features for the 1 : 13 composition are rather clearly seen in both curves. We also studied the nitric acid—water (see Fig. 5, *b* and Fig. 9, curve *2*) and (in less detail) hydrochloric acid—water systems (see Fig. 9, curve *3*). For the HNO_3—H_2O system, a pronounced specific feature was observed for the 1 : 16 composition

* The chemical shifts relative to liquid water are denoted by the letter *S*.

at 0 °C and several, less pronounced, features were found at higher temperatures.

A comparison with the data for the $HClO_4$—H_2O system led us to conclude that at temperatures below 30 °C, aqueous solutions of nitric acid exist as quasi-ideal mixtures of neat water and the solvation structures $\{[(H_3O^+)\cdot 3H_2O]\cdot 9H_2O\}(NO_3^-)\cdot 3H_2O$ up to the 1 : 16 composition. The situation becomes more complicated with increasing temperature due to the appearance of structures containing a larger number of water molecules. At temperatures below 30 °C, the proton is present as the solvation ion H_3O^+ in all three aqueous acid systems under study, whereas it exists as the solvation ion $H_5O_2^+$ at temperatures above 40 °C.

From the above, the following conclusions can be drawn.

1. Plots of the chemical shifts of aqueous-acid systems *vs.* the composition have specific features observed as gently sloping regions and inflection points in the plots of the derivative with respect to the linearization coordinate, which provide information on the solution structure.

2. At temperatures below 30 °C, the higher proton hydrate has the 1 : 13 composition and contains H_3O^+ in the center; at temperatures above 40 °C, the prevailing hydrate has the composition ~1 : 30 and is $H_5O_2^+$-centered.

3. Proton hydrates are linked to the environment by H bonds, whose characteristics are similar to those in pure water.

4. Changes in the proton chemical shifts depending on the composition correlate with the changes in the density.

Finally, the temperature region in the vicinity of 30 °C is critical from the point of view of not only our data on proton hydration but also of the data on many other properties of liquid water, in particular, the viscosity, the heat capacity c_p, the nuclear spin-lattice relaxation, *etc.*[63]

3.2. Solutions of nitrates in nitric acid. *The N_2O_5—HNO_3 system.* It is known[64] that 100% nitric acid undergoes partial self-dissociation:

$$2\,HNO_3 \rightleftharpoons \overbrace{H_2O + NO_2^+ + NO_3^-}^{\sim 1.5\ mol.\%}$$

However, the equilibrium in N_2O_5 solutions in nitric acid is shifted to the left and HNO_3 exists almost completely in the molecular form. At the same time, as follows from the data published earlier,[65] the amount of nondissociated N_2O_5 is negligible, and it can be assumed that the system in question consists of HNO_3 molecules and NO_2^+ and NO_3^- ions solvated by the acid.

The plot of the integral heat of solution (ΔH_s°) for N_2O_5 (sol.) in HNO_3 (liq.) *vs.* the N_2O_5 concentration per mole of HNO_3 [48] (N_2O_5 concentration is given in molality L, $T = 298.15$ K) is presented in Fig. 11 (curve *1*).

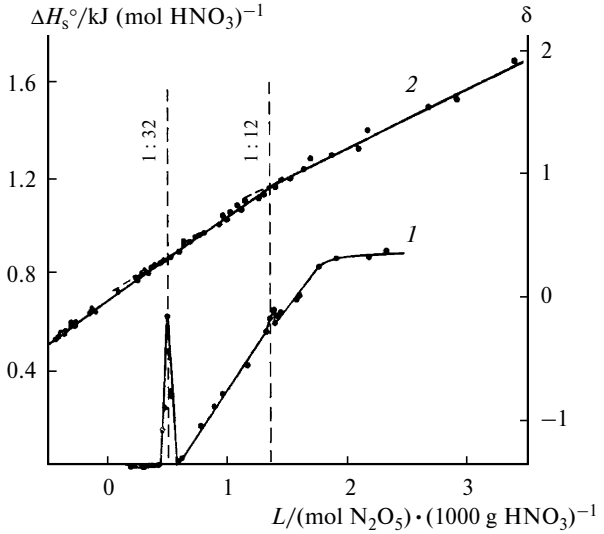

Fig. 11. Concentration dependence of the integral heat of solution (ΔH_s°) of N_2O_5 (sol.) in HNO_3 (liq.) at 25 °C[48] (*1*) and the proton chemical shifts (δ) in the N_2O_5—HNO_3 system at 20 °C (*2*); the chemical shifts were converted relative to H_2O as the internal standard. The correlation coefficients for the straight lines approximating the chemical shifts are 0.999, 0.985, and 0.994 for three regions in the order of increasing L.

The heat of solution increases with increasing N_2O_5 concentration. Noteworthy is a narrow peak at $L \approx 0.5$ (N_2O_5—HNO_3, 1 : 32): $\Delta H_s^\circ = 20.9$ kJ mol^{-1} per mole of N_2O_5 (or 0.63 kJ mol^{-1} per mole of HNO_3). A small peak is observed for $N_2O_5 : HNO_3 = 1 : 12$. The maximum in the concentration dependence of the heats of mixing is generally evidence for the formation of the reaction product of the starting compounds *via* intermolecular bonds. However, in the case under consideration, the presence of a large number of solvation molecules in such a "product" and the unusually narrow region, in which the maximum appears (only 1.5 mol.%), are indicative of the manifestation of the effects of the solution structure.

To verify this assumption, the concentration dependences of the ^1H, ^{14}N, and ^{17}O NMR parameters were studied in detail.[48] The results are presented in Fig. 11 (curve *2*) and Fig. 12.

All these spectra show one signal averaged due to fast chemical exchange processes:

$$(n+m)\,HNO_3 + N_2O_5 \rightleftharpoons \rightleftharpoons NO_3^-\cdot n HNO_3 + NO_2^+\cdot m HNO_3, \qquad (9)$$

$$(NO_3^-)^* + HNO_3 \rightleftharpoons H(NO_3)^* + NO_3^-.$$

In all cases, the N_2O_5 concentration in solution is plotted on the abscissa in such units that the abscissa serves as the linearization coordinate with respect to which the corresponding parameters are linear in the regions between the inflection points. It can easily be demonstrated[14,15,43] that the molality L has this property for the

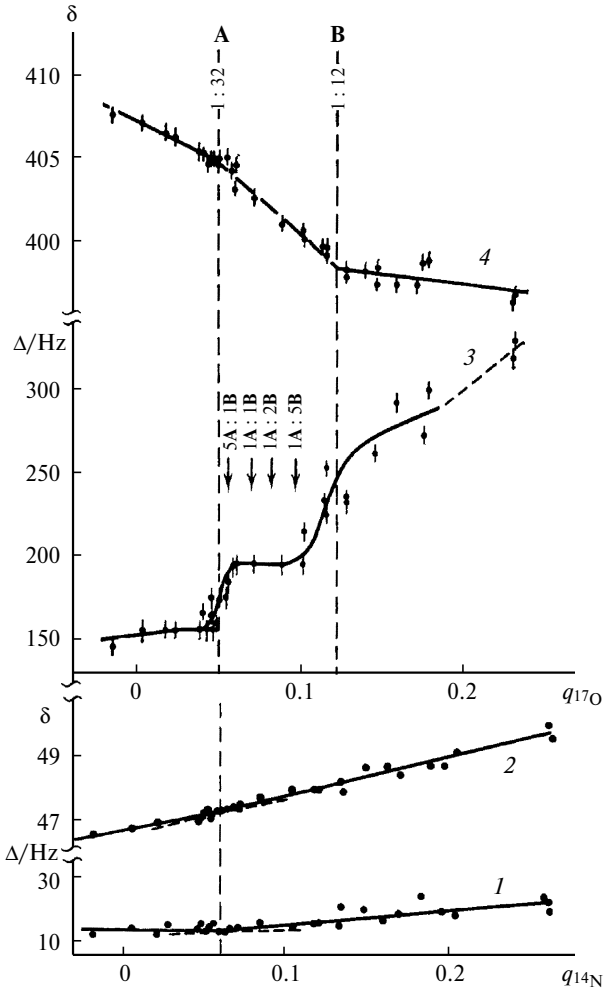

Fig. 12. Dependences of the chemical shifts (δ) and the linewidth (Δ) of the average ^{14}N NMR signals (*1*, *2*) at 25 °C and ^{17}O NMR signals (*3*, *4*) at 20 °C on the composition of the N_2O_5—HNO_3 system (^{14}N chemical shifts are given relative to $MeNO_2$ as the external standard, and the ^{17}O chemical shifts are given relative to H_2O as the external standard). The correlation coefficients for the approximating straight lines are 0.963 and 0.974 for δ and 0.465 and 0.825 for Δ for the regions $q_N < 0.06$ and $q_N > 0.06$, respectively.

proton chemical shifts, and $q_{^{14}N} = 2x/(1 + x)$ and $q_{^{17}O} = 5x/(2x + 3)$ (x is the molar fraction of N_2O_5) serve as this property for the average ^{14}N and ^{17}O NMR signals, respectively.

It is reasonable to expect that the sensitivity of the NMR parameters to the changes in the solution structure depends on the type of nuclei, which is confirmed by Figs 11 and 12. Studies of the proton chemical shifts for a number of systems showed[14,15,43] that the changes in the slope at inflection points are generally small, which imposes high requirements on the measurement accuracy. The accuracy of the results of ^1H and ^{14}N NMR experiments appeared to be insufficient to unambiguously find fine specific features of the concentration dependences. Meanwhile, it is possible to make an approximation of the linear-bent curve with inflection points for the 1 : 32 and 1 : 12 compositions for the proton chemical shifts and an inflection point for the 1 : 32 composition for the ^{14}N NMR parameters (see Fig. 11, curve *2* and Fig. 12, curves *1* and *2*). The scatter in the experimental points is much larger than the measurement error and is attributed to the influence of paramagnetic decomposition products* (O_2 and NO_2). As can be seen from Fig. 12 (curves *3* and *4*), the ^{17}O resonance is more sensitive to the structural changes in solution. The plot of the chemical shifts has a pronounced linear-bent character and is characterized by inflection points for the 1 : 32 and 1 : 12 compositions corresponding to the large and small peaks, respectively, in the curve of the heat of mixing (see Fig. 11).

As expected, the width (Δ) of the averaged quadrupole ^{17}O signal in electrolyte solutions,[45] which is determined by the quadrupole relaxation rates substantially increases with increasing N_2O_5 concentration. However, the plot is wave-like rather than linear-bent, which is generally observed for such dependences, and sharp changes alternate with more gently sloping regions, the concentration regions characterized by a sharp change in the linewidth in the vicinity of the 1 : 32 and 1 : 12 compositions being identical to the concentration regions, where the peaks in the curve of the heat of mixing are observed. In our opinion, particular prevailing diffusion-averaged solvation structures correspond to the 1 : 32 and 1 : 12 compositions, whereas there is a dynamic equilibrium between two structures at concentrations higher and lower than these compositions.

Certain information on these structures can be obtained from the data[64] on the electronic structures of the NO_2^+ and NO_3^- ions and their properties as solvation centers in HNO_3 [66] and taking into account the principle of the construction of solvation complexes in H-bonded solvents found for such systems.[14,15,43] The NO_3^- ions are symmetric planar and contain partially double N⋯O bonds and two lone electron pairs at sp^2-hybridized oxygen atoms. These lone electron pairs are efficient proton acceptors. The NO_3^- ion would be expected to form strong H bonds in proton-donor media, including HNO_3, which is confirmed by the existence of the crystal solvates $MNO_3 \cdot nHNO_3$, where n = 1, 2, or 3 [66] (M is the metal atom). If solvation complexes are constructed based on the number of vacancies for H bonding,[14,15,43] we obtain the maximum solvation number of 18 for NO_3^- (6 and 12 in the first and the second coordination spheres, respectively) (Fig. 13). The NO_2^+ counterion is linear and contains double N=O bonds.[64] The electron density distribution in this counterion is such that the nitrogen atom

* For concentrations $L > 1$, the proton chemical shifts increase by several Hertzs during measurements; the observed chemical shifts were extrapolated to the instant of mixing.

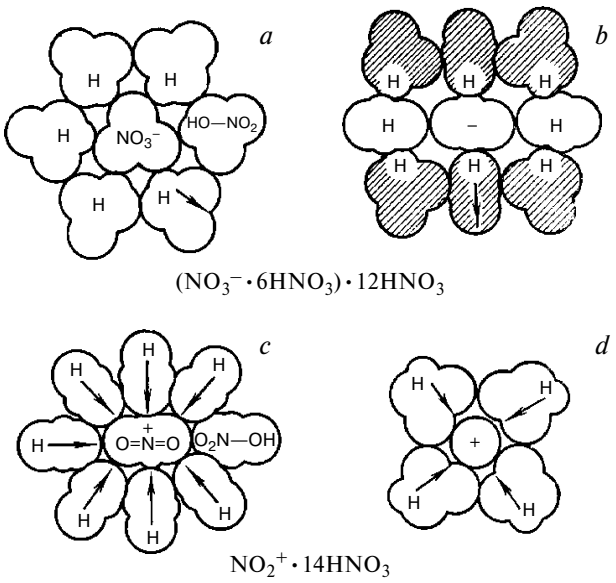

Fig. 13. Schematic representation of the fragments of the solvation complex $N_2O_5 \cdot 32HNO_3$: *a*. The cross-section of the solvation complex $NO_3^- \cdot 18HNO_3$ by the plane passing through the plane of the ion. Only the first solvation shell is shown, the second solvation shell is located above and below the plane of the figure; *b*. The cross-section of the same solvation complex by the plane, which is perpendicular to the plane of the ion and passes through one of the N⋯O bonds. A part of the first solvation shell (undashed HNO_3 molecules) and one-half of the second solvation shell (dashed HNO_3 molecules) are shown. *c*. The cross-section of the solvation complex $NO_2^+ \cdot 14HNO_3$ by the plane, which passes through the line that links the O, N, and O atoms; *d*. The cross-section of the same solvation complex by the plane, which is perpendicular to the line passing through the O, N, and O atoms and passes through the center of the solvation complex. The direction of the dipole moments of the HNO_3 molecules are indicated by arrows. The cross-sections of the ions and HNO_3 molecules are shown taken into account the ratios of the van der Walls radii of the H, N, and O atoms.

bears a positive charge of +0.6 e, and the charge on the oxygen atoms is +0.2 e.[67] In the solvation NO_3^- complexes, where solvation occurs *via* H bonds, the direction of the dipole moments of the HNO_3 molecules (dipole moments are 2.16 D) corresponds to the maximum electrostatic interactions between the dipoles and the ion, resulting in the increase in the degree of solvation. In the case of the NO_2^+ ion, the dipole contribution and the contribution of H bonds act in opposite directions (see Fig. 13), which should lead to a weakening of solvation. Since the oxygen atoms in the NO_2^+ ion bear a positive charge that hinders H bonding, solvation of NO_2^+ most probably occurs according to the dipole mechanism. Since the higher solvation complex of two counterions generated from the N_2O_5 molecule contains 32 HNO_3 molecules, the solvation shell of NO_2^+ contains 32 – 18 = 14 HNO_3 molecules, which is quite consistent with the coordination number for the close packing (see Fig. 13). In the solvation structure corresponding to the 1 : 12 composition, only the first coordination sphere about the NO_3^- ion and the partially dipole shell of NO_2^+ are, apparently, retained, so that the counterions in the resulting structure remain solvate-separated.

Unfortunately, the published data on the concentration dependences of other physicochemical properties of the system in question (density,[68] viscosity, surface tension,[69] conductivity,[68] melting point,[68,70] heat capacity,[69] thermal decomposition rate,[71] *etc*.) are insufficient to reveal the correlation with the fine effects of liquid structuration, because the intervals between the experimental points are large, and the results of measurements in the vicinity of the 1 : 32 and 1 : 12 compositions are lacking. It should be noted that, according to the published data,[68] the slopes of the concentration plots for the conductivity and the heat capacity sharply change in the vicinity of the 1 : 12 composition.

Let us consider in more detail the relationship between the structure of a N_2O_5 solution in HNO_3 and the character of the specific features of the concentration plots for the heats of mixing and the ^{17}O NMR linewidths. The heat of mixing (see Fig. 11) reflects the total change in the enthalpy of intermolecular interactions in solution compared to individual compounds. In the case of small changes in the composition in the region, where the peak of ΔH_s is observed, the heat of solution $\Delta\Delta H_s^\circ$ can be represented as follows: $\Delta\Delta H_s^\circ = \Delta E_{inter} \approx \Delta E_{H_b} + \Delta E_{coul} + \Delta E_{vdw}$, where ΔE_{inter} is the total energy change of intermolecular interactions, ΔE_{H_b} is the energy change of H bonds, ΔE_{coul} is the energy change of electrostatic interactions (ion—ion, ion—dipole, and dipole—dipole), and ΔE_{vdw} is the energy change of van der Waals interactions (orientation, polarization, and dispersion interactions). The proton chemical shifts (see Fig. 11) reflect the contribution of the H-bond energy to the total energy of intermolecular interactions. Assuming that the excessive heat released in the vicinity of the peak is totally associated with the changes in the H-bond network and taking 0.26 ppm mol kJ^{-1} for the proportionality coefficient between the proton chemical shifts and the H-bond energy (see Refs 40 and 72), we obtain that the maximum expected change in the proton chemical shift is 0.13 ppm. As can be seen from Fig. 11, the maximum heat of mixing for the 1 : 32 composition cannot be assigned to a strengthening of H bonds in the system because the peak in the plot of the chemical shifts is absent in this concentration range. Consequently, a decrease in the internal energy of the system is attributed to a strengthening of another type of intermolecular interactions (electrostatic or van der Waals). The 1 : 32 solvation structure is favorable from the standpoint of these intermolecular interactions (apparently, even between solvation complexes), whereas the presence of an impurity of other solvation forms decreases

the interaction energy. It should be noted that the peaks of the heats of mixing and the regions of sharp changes in the ^{17}O NMR linewidth are at the boundaries of the linear regions in the plots of the chemical shifts *vs*. the composition, in the vicinity of inflection points, and correspond to a sharp change in the proportion of the solvation forms. Let us denote the 1 : 32 and 1 : 12 solvation forms as **A** and **B**, respectively. The **B** : **A** ratio varies from 1 : ∞ at the center of the peak to 1 : 5 at the boundaries (see Fig. 12). In the middle of the linear regions, where the proportion of the solvation forms varies approximately from 1 : 5 to 5 : 1, the concentration dependence of the properties is more gently sloping.

Taking into account this character of changes in the solution structure, the jumps in the linewidth $\Delta = 1/\pi T_2$ (T_2 is the spin-spin relaxation time of ^{17}O nuclei) can be attributed to a substantial contribution of the scalar relaxation of the first kind $\Delta_{sc} = (1/\pi T_2)_{sc}$ from fast exchange processes.[73] Let us assume that in this case, the rate of exchange processes is also determined by the rate of the so-called structural diffusion,[18] *i.e.*, the rearrangement of the liquid structure into the structure of the solvation complex of the corresponding ion. In this case, when the system is a mixture of the solvation complexes **A** and **B**, the structural diffusion consisting in the intersolvent rearrangement can be represented as a combination of the following reactions:

$$\mathbf{A} + \mathbf{A} \overset{k_1}{\rightleftharpoons} \mathbf{A}^* + \mathbf{A}^*,$$

$$\mathbf{A} + \mathbf{B} \overset{k_2}{\rightleftharpoons} \mathbf{A}^* + \mathbf{B}^*,$$

$$\mathbf{B} + \mathbf{B} \overset{k_3}{\rightleftharpoons} \mathbf{B}^* + \mathbf{B}^*,$$

where k_1, k_2, and k_3 are the rate constants of the corresponding exchange processes, and the asterisk means that the solvation complex undergoes a rapid chemical exchange according to Eqs (9). The contribution of these exchanges to the linewidth can be estimated according to the equation[73] $\Delta_{sc} = (1/\pi T_2)_{sc} \approx 1/\tau_{ex}$, where $1/\tau_{ex}$ is the rate of the exchange process, which can be represented as follows:

$$1/\tau_{ex} = k_1[\mathbf{A}]^2 + k_2[\mathbf{A}][\mathbf{B}] + k_3[\mathbf{B}]^2$$

([**A**] and [**B**] are the concentrations of the corresponding solvation forms). Then the total linewidth, which is equal to the sum

$$\Delta = 1/(\pi T_1) + [1/(\pi T_2)_{sc}],$$

(T_1 is the spin-lattice relaxation time of quadrupole ^{17}O nuclei), can be characterized by the concentration dependence more complicated than the linear-bent dependence observed in the case of $T_1 = T_2$.

Therefore, the detailed study of certain physicochemical properties of the N_2O_5—HNO_3 system demonstrated that the ^{17}O NMR parameters and the heats of mixing are very sensitive to fine specific features of the solution structure. A comparison of the results for the N_2O_5—HNO_3 system with the data obtained earlier[14,15,43] for other solutions of strong electrolytes showed that the dynamic equilibrium between pairs of thermodynamically stable diffusion-averaged solvation structures giving rise to linear regions and inflection points in the concentration plots for certain properties has a rather general character. A new fact is that the anomalies were observed as sharp changes not only in the derivatives of the properties but also in the properties as such at the point when one pair of structures is transformed into another pair, *i.e.*, in the vicinity of the compositions, where one solvation form predominates. The nature of these anomalies remains unclear. Apparently, they are related to the ordering of the solvation complexes due to association and are similar to the structural phase transitions in liquids.[74]

In conclusion, it should be noted that the structuration effects in liquid electrolyte solutions are, apparently, widespread. In particular, they should be taken into account in the consideration of chemical transformations sensitive to solvation. An example of such transformations is given below.

The MNO_3—HNO_3 system. In MNO_3 solutions in HNO_3, like in the N_2O_5—HNO_3 system, nitric acid exists in the molecular form.[48,64,66] In this case, the acid molecules, which have proton-donor and proton-acceptor properties and the dipole moment of 2.16 D, also solvation NO_3^- anions *via* H bonds and ion—dipole interactions.[48] All NMR spectra also show single signals averaged due to the following fast exchange processes:

$$(m + n)\,HNO_3 + MNO_3 = \\ = NO_3^- \cdot n HNO_3 + M^+ \cdot m HNO_3, \qquad (10)$$

$$(N^*O_3)^- + HNO_3 = HN^*O_3 + NO_3^-. \qquad (11)$$

Unlike the N_2O_5—HNO_3 system, solutions of alkali metal nitrates in HNO_3 are rather stable. This made it possible to improve the measurement accuracy,[49] which is particularly important for the proton resonance. Concentration* dependences of δ_H for the Na, K, and Cs systems in the regions of their solubility for two temperatures are shown in Figs 14 and 15. The specific features were found with the use of the difference derivative methods, which give the most reliable results.[43] Like for other systems,[15,43,48] the plots of the derivative with respect to the linearization coordinate, $\Delta\delta/\Delta L$ (L is the molality), appear as typical smoothed-out steps. This situation corresponds to the linear-bent character of $\delta(L)$. Smoothing is partially due to the procedure used for tak-

* In all cases, the linearization coordinate q was used as the concentration; the corresponding parameters are linear relative to this coordinate in the regions between the inflection points.

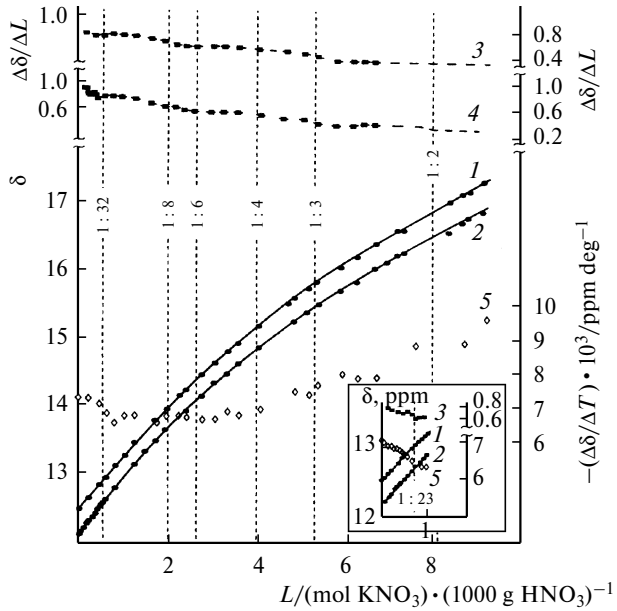

Fig. 14. Concentration dependence of the ^{1}H NMR parameters for the KNO_3—HNO_3 system: δ relative to Me_4Si as the internal standard (*1*, *2*), $\Delta\delta/\Delta L$ (*3*, *4*) at −25 (*1*, *3*) and 22 °C (*2*, *4*) and $\Delta\delta/\Delta T$ (*5*). The data for the $NaNO_3$—HNO_3 system are given in the inset: δ (*1*, *2*), $\Delta\delta/\Delta L$ (*3*) at −26.5 (*1*, *3*) and 22 °C (*2*) and $\Delta\delta/\Delta T$ (*5*).

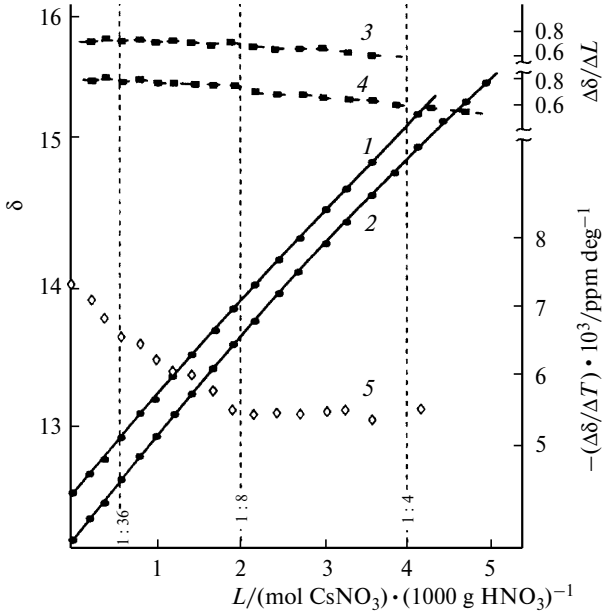

Fig. 15. Concentration dependence of the ^{1}H NMR parameters for the $CsNO_3$—HNO_3 system: δ relative to Me_4Si as the internal standard (*1*, *2*), $\Delta\delta/\Delta L$ (*3*, *4*) at −26.5 (*1*, *3*) and 22 °C (*2*, *4*) and $\Delta\delta/\Delta T$ (*5*).

ing the difference derivative.[43] The inflection points for $\Delta\delta/\Delta L$ correspond to the inflection points for $\delta(L)$. Although the observed effects are weakly pronounced, the inflection points for the 1 : 8 compositions can reliably be determined both for the K and Cs systems. For the K system, there are also, apparently, inflection points for the 1 : 4 and 1 : 3 compositions and, probably, for the 1 : 6 and 1 : 2 compositions. These figures show also the temperature coefficients of $\Delta\delta/\Delta T$ determined from the results of measurements at two temperatures. The 1 : 4 (for the K system) and 1 : 8 (for the Cs system) compositions are specific also for this parameter. At these points, the changes in the slope of the concentration plot for $\Delta\delta/\Delta T$ are observed. The concentration plots for $\Delta\delta/\Delta L$ and $\Delta\delta/\Delta T$* of the three systems in question provide evidence that there are also specific features in the concentration region, where there are 20—40 moles of the acid per mole of the salt, *i.e.*, in the concentration region called by the boundary of complete solvation,[75] and the pronounced specific features are observed for the N_2O_5—HNO_3 system (for the 1 : 32 composition) in the ^{17}O NMR spectrum and the heats of mixing. However, these effects are weak, and reliable results were not obtained. The concentration plots for the proton chemical shifts for all the systems under study, including N_2O_5—HNO_3, are similar, which confirms the conclusion[48] that H bonds play the decisive role in solvation NO_3^- complexes.

According to the general concepts of NMR spectroscopy, the average proton chemical shift in these systems is

$$\delta_H = \Sigma p_i \delta_i, \qquad \Sigma p_i = 1, \tag{12}$$

where δ_i are the chemical shifts and p_i are the probabilities of the occurrence of the acid molecules in different states. From Eq. (12), taking into account Eqs (10) and (11), for the initial region of the concentration dependence (up to the first inflection point), we obtain

$$\delta_H = \{mL\delta_+ + nL\delta_- + [N - L(m+n)]\delta_0\}/N, \tag{13}$$

where $N = 1000/63$, the plus and minus signs refer to the solvation cation and anion complexes, respectively, and zero corresponds to the bulk of the solvent.

Let us use the concept of the total proton chemical shift of solvation complexes (S_Σ),[43] which characterizes the H-bond energy excessive relative to the bulk of the solvent, to characterize the solution structure. In the general case, without the separation of the solvent between the cations and anions, we have the following equation for solvation structures at singular points:

$$S_{\Sigma,j} = Z_j(\delta_j - \delta_0), \tag{14}$$

where Z_j is the number of moles of the solvent per mole of the dissolved compound in the jth solvation structure,

* Under the conditions of an external standard, $\Delta\delta/\Delta T$ is determined with higher accuracy than $\Delta\delta/\Delta L$, because errors due to the nonidentity of resonating cells in a series of samples are excluded.

Table 3. Total proton chemical shifts (S_Σ) in solvation complexes relative to the corresponding solvent[15,43,48,49]

System	Higher solvation complex	S_Σ, ppm (T/°C)
$HClO_4$—H_2O	1 : 13	28.5 (35)
HNO_3—H_2O	1 : 16	33.5 (22)
HCl—H_2O	—	36 (22)
HCl—N_2H_4	1 : 6	26.8 (100)
HCl—Me_2NNH_2	1 : 6	21.3 (64)
HCl—MeHNNHMe	1 : 4	22.3 (74)
$NaNO_3$—HNO_3	~1 : 30	12.5 (22)
KNO_3—HNO_3	~1 : 30	14.4 (22)
$CsNO_3$—HNO_3	~1 : 30	12.3 (22)
N_2O_5—HNO_3	1 : 32	11.2 (20)

and δ_j is the average proton chemical shift in this structure. For a higher solvation complex, assuming $j = 1$, we obtain the following equation from Eqs (13) and (14)

$$S_{\Sigma,1} = Z_1(\delta_1 - \delta_0) = N(d\delta_H/dL|_{L\to 0}) = \\ = m\delta_{1+} + n\delta_{1-} - (m+n)\delta_0. \quad (15)$$

The chemical shifts S_Σ calculated from Eq. (15) for a number of systems studied earlier[15,43,48,49] are given in Table 3. As can be seen from Table 3, the total proton chemical shift for the higher solvation complex in nitrate solutions in nitric acid relative to the chemical shift in the bulk of the solvent, which is determined predominantly by anion solvation, is substantially lower than S_Σ in aqueous and hydrazine solutions of acids, where the chemical shift refers predominately to the proton solvation complex, whereas the solvation anion complex is responsible only for the difference in S_Σ in solutions of different acids. Hence, it follows that, although the H-bond energies in nitrate solutions in nitric acid are high, the concentration of the excessive H-bond energy in solvation NO_3^- complexes compared to the bulk of the solvent is much lower than that for the proton solvation complex in water but is higher than that for the solvation NO_3^- complex in water.

In the general case, this corresponds to the commonly accepted concepts. The following ΔE_{H_b} can be obtained for the excessive H-bond energies in the solvation complexes $H^+ \cdot 13H_2O$, $NO_3^- \cdot nH_2O$, and $NO_3^- \cdot 18HNO_3$ from the relationships between the chemical shifts and the H-bond energy:[40] ~130, ~ 21, and 56.5±6 kJ mol^{-1}, respectively.

The ^{14}N NMR spectroscopic data for the K system (Fig. 16) are consistent with the ^{1}H NMR data. The signal is shifted downfield by ~20 ppm with increasing salt concentration and is accompanied by small deviations from the linearity, which corresponds to an increase in the contribution of NO_3^-. The chemical shift of this signal in nitric acid relative to HNO_3 is 52 ppm,[76] which is similar to the corresponding value in water.[66] The opposite direction of the shift of the averaged ^{14}N signal in the

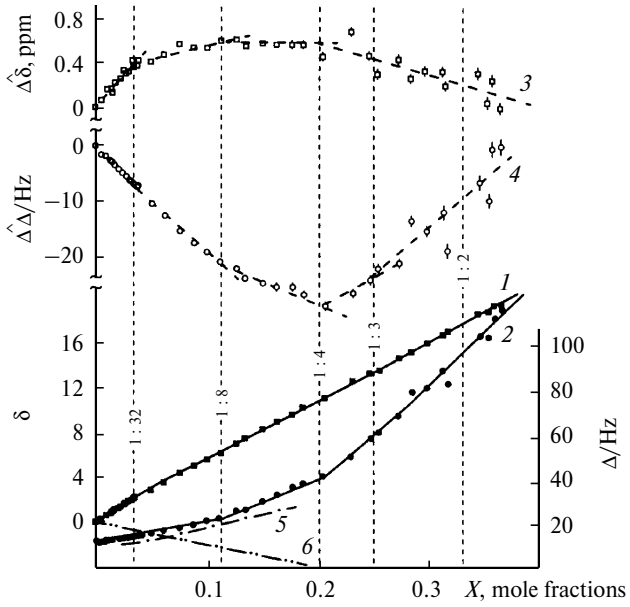

Fig. 16. Concentration dependence of the ^{14}N NMR parameters for the KNO_3—HNO_3 system at 25 °C: δ relative to HNO_3 as the internal standard (*1*), Δ (*2*), $\hat{\Delta}\delta$ (*3*), and $\hat{\Delta}\Delta$ (*4*) are the deviations of the observed shifts δ and Δ from the straight lines passing through the extreme experimental points (see the text) and for the N_2O_5—HNO_3 system at 20 °C:[48] δ relative to HNO_3 as the internal standard (*5*) and Δ (*6*).

HNO_3—N_2O_5 system is attributed to the presence of yet another particle (NO_2^+ cation) involved in the exchange. The chemical shift of this cation in ^{14}N NMR spectra, which was estimated on the assumption that the chemical shift of the NO_3^- anion in the KNO_3—HNO_3 system is identical to that in the N_2O_5—HNO_3 system, is −88 ppm relative to HNO_3 and agrees well with the chemical shift of −83 ppm (see Ref. 66).

The linewidth of the averaged ^{14}N signal in the KNO_3—HNO_3 system changes from 10 to 120 Hz with increasing concentration, which can be caused by an increase in the asymmetry of the environment of the ^{14}N nucleus, an increase in the quadrupole coupling constants, and retardation of motion of the surrounding particles.

Since the difference derivative method cannot be used for revealing the specific features of the concentration dependences of the chemical shifts and Δ because of the insufficient measurement accuracy, we attempted to use the method of deviations of the observed values from straight lines passing through the extreme experimental points. This method makes it possible to more descriptively represent the linear-bent approximation. As can be seen from Fig. 16, both concentration dependences can be approximated by linear-bent curves whose inflection points are identical to those observed in proton resonance (1 : 4, 1 : 8, and ~1 : 30).

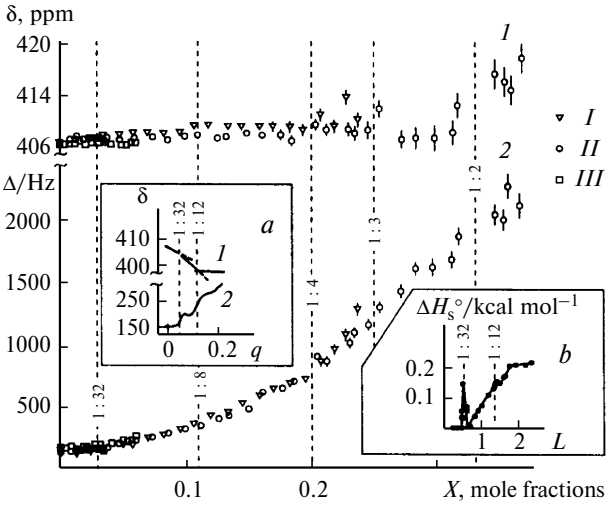

Fig. 17. Concentration dependence of the ^{17}O NMR parameters for the MNO_3—HNO_3 systems for M = Cs (*I*), K (*II*), and Na (*III*) at 20 °C: δ relative to H_2O as the external standard (*1*) and Δ (*2*). The inset *a* shows the data for the N_2O_5—HNO_3 system at 25 °C: δ (*1*) and Δ (*2*) relative to the corresponding linearization coordinate *q*, the inset *b* shows the concentration dependence of the integral heat of solution for N_2O_5 (sol.) in HNO_3 at 25 °C.[48]

Let us consider the concentration dependences of the chemical shifts and linewidths of ^{17}O NMR signals for all the systems in question (Fig. 17). In this case, ^{17}O NMR spectroscopy appeared to be poorly informative as opposed to the data for the N_2O_5—HNO_3 system, for which pronounced specific features were observed as a linear-bent plots for δ and jumpwise changes in Δ for the 1 : 32 and 1 : 12 compositions. It can be seen that the chemical shifts weakly depend on the nitrate concentration and are similar for all systems. The ^{17}O chemical shift of the NO_2^+ cation estimated under the same assumptions as for the ^{14}N chemical shift is δ −200 relative to 100% HNO_3. The concentration plot for the linewidth is also virtually identical for all nitrates, although a very strong broadening is observed (from 150 to 2000 Hz). It should be noted that the plot of $\Delta(X)$ for the N_2O_5—HNO_3 system passes slightly lower, *i.e.*, the additional contribution of the oxygen atoms of the NO_2^+ group leads to a decrease in the relaxation rate $1/T_2 = \pi\Delta$. The observed linewidths are much larger than those typical of low-molecular-weight compounds (≤500 Hz)[73] and cannot, apparently, be attributed exclusively to an increase in the quadrupole coupling constants due to an increase in the electric field gradients, but are indicative of an increase in the correlation time of the particle motion. Presumably, this increase is associated with retardation of proton fluctuations[76] in H bonds between NO_3^- and the solvating HNO_3 molecules, although the exchange remains fast on the NMR time scale.

For completeness, the ^{23}Na and ^{133}Cs NMR spectra in the corresponding systems were also studied. The ^{23}Na NMR signal is shifted upfield by ~1 ppm with increasing nitrate concentration, the line being broadened from 10 to 20 Hz, which is indicative of a rather symmetric environment of the cation and its insignificant change in the concentration range under study. The ^{133}Cs chemical shifts are shifted downfield by ~20 ppm with increasing nitrate concentration with $\Delta \ll 1$ Hz throughout the concentration range. Taking into account the quadrupole moment of the ^{133}Cs nucleus, this fact confirms high symmetry of the environment (most likely, due to fast rotation of the Cs^+ ion). The linearization coordinate for both nuclei is $(1 - X)/X$. However, although the experimental points can be approximated by the linear-bent curve with the 1 : 4 and 1 : 8 inflection points for Cs and the 1 : 23 and 1 : 35 inflection points for Na, the effects under consideration are not sufficiently convincing.

Therefore, the investigation of these systems confirms, on the whole, that the linear-bent character of the concentration dependences of the NMR parameters (which reflects[14,15,43,48] the dynamic equilibrium between pairs of the prevailing diffusion-averaged solvation structures) is a common property of electrolyte solutions in H-bonded systems. The degree of manifestation of such specific features in different systems depends on the type of NMR spectra and NMR parameters. In some cases, rather convincing results were obtained, although these effects are generally weak. The ^1H NMR spectroscopic data, which are represented as the concentration dependences of the difference derivative and the temperature coefficient of the chemical shift, are most reliable. The temperature coefficient, which is determined with higher accuracy and excludes the regular smearing of the inflection region typical of the difference derivative of the chemical shift,[43] is particularly important for the precise determination of the compositions of the prevailing structures.

Unfortunately, attempts to determine the precise compositions of higher solvation structures, which are analogous to the 1 : 32 structure in the N_2O_5—HNO_3 system, in these systems failed. In the case under consideration, the solvation structures with the 1 : 8 and 1 : 4 compositions in the K and Cs systems, which were rather reliably determined, do not follow the rule of filling of all vacancies for H bonding in the coordination spheres about ions as was observed in aqueous and hydrazine solutions of acids.[14,15,43,48] Apparently, this difference is attributed to the changes in the relative role of the contributions to the intermolecular interaction energy

$$\Delta E_{inter} = \Delta E_{H_b} + \Delta E_{coul} + \Delta E_{vdw},$$

or, to be more precise, to the fact that the H bond component ΔE_{H_b} does not have a dominant role as opposed to aqueous and hydrazine solutions of acids, whereas the

role of the Coulomb (ΔE_{coul}) and van der Waals (ΔE_{vdw}) interactions increases. This is quite consistent with the lower excessive H-bond energies in solvation structures compared to those in solutions of acids (see Table 3).

The temperature coefficient of the proton chemical shift in H-bonded systems is related in a complex way to the structure and reflects the average change in the number and energy of H bonds. The concentration dependences of the temperature coefficient of the chemical shift for the systems described in the study[49] were compared with those of $HClO_4$ solutions in H_2O studied earlier,[43] where $\Delta\delta/\Delta T$ monotonically decreases with increasing concentration of the acid, based on simple concepts,[43] which relate the changes in $\Delta\delta/\Delta T$ to the changes in the proportions of arbitrarily "strong" and "weak" H bonds in systems. This comparison shows that the proportion of "strong" H bonds in nitrate solutions in HNO_3 slightly increases, then remains constant, and finally decreases with increasing electrolyte concentration. Under the assumptions used, estimations demonstrated this behavior of $\Delta\delta/\Delta T$ to indicate that structures, in which six H bonds between the NO_3^- group and the adjacent HNO_3 molecules are equivalent and "strong," are transformed into structures, in which only three or one bond can be considered as "strong," whereas other bonds are "weak," which leads to an increase in $\Delta\delta/\Delta T$.

The available data provide evidence that all the systems in question, including N_2O_5—HNO_3, have similar structures throughout the concentration range under study. In the concentration range up to the ~1 : 30 composition, the solvation anion and cation complexes exist separately as $NO_3^- \cdot 18HNO_3$ and $M^+ \cdot mHNO_3$ (m is the coordination number).[48] The cation is solvated *via* ion—dipole interactions according to the principle of close packing,[48] whose occurrence in this case, as opposed to solutions in H_2O, is not hindered by the solvent structure. The coordination numbers determined with the use of the molecular models and the experimental data for aqueous solutions[52] are given in Table 4. In the solvation NO_3^- complex, the arrangement and orientation of HNO_3 molecules are such that the direction of the dipole moments of the acid molecules in the case of solvation *via* H bonds corresponds to the maximum ion-dipole contribution,[48] resulting in an increase in the degree of solvation of the anion compared to the cation. The latter fact is confirmed by higher solubility of nitrates in HNO_3 (dielectric permeability $\varepsilon = 50$) than in H_2O ($\varepsilon = 80$) and the reverse dependence of the solubility on the cation size. In water, the solubility of alkali metal nitrates decreases with increasing cation radius (dominant solvation of the cation occurs), whereas the solubility in nitric acid increases, although potassium nitrate drops out of the series toward higher solubility.

Table 4. Diameters (d) and coordination numbers (m) of the cations in HNO_3 and H_2O

Cation	d/Å	m	
		HNO_3	H_2O (see Ref. 52)
Li^+	1.20	—	4—7
Na^+	1.90	5	5—7
K^+	2.66	7	7—8
Cs^+	2.96	10	5—8
NO_2^+	3.16×5.40*	14	—

* The transverse and longitudinal sizes of the ion.

The schematic representation of the assumed structures is presented in Fig. 18. In the case of the favorable geometric relationships, which apparently take place in the N_2O_5—HNO_3 system, higher solvation cation and anion complexes can be closely packed to form a thermodynamically stable diffusion-averaged structure. This leads to the appearance of singular points in the concentration curves of the NMR parameters and other physicochemical properties for the 1 : ($m + n$) ratio of the salt concentration to the acid concentration. If the geometric relations are unfavorable, *i.e.*, higher solvation complexes "are not packed," the structural rearrangements frequently occur in this concentration range and the pattern is smeared, which is, apparently, occurs for M = Na, K, and Cs. It should be noted that the shape and size of the cations, *viz.*, alkali metal ions (unlike NO_2^+), allow these cations to be included in the cavities formed by the solvation anion complexes (see Fig. 18, **II**). In this case, the number of cavities is larger than the number of cations, which is also the reason why the compositions of the prevailing structures are not pronounced. The 1 : 8 solvation structures of the K and Cs systems are, apparently, analogous to the 1 : 12 structure for the N_2O_5—HNO_3 system,[48] and a decrease in the number of HNO_3 molecules is associated with a decrease in the cation size. The 1 : 4 structure is similar in composition to the 1 : 1 and 1 : 2 crystal solvates known[64] for these systems.

In the concentration range, where the solvation shells of the ions overlap, the prevailing structures correspond to special points in the concentration curves for the NMR parameters have diffusion-averaged ideal configurations, which include the counterions and solvent molecules arranged in a particular fashion. Being liquid-phase analogs of unit cells in crystals, these particles are essentially "unit cells" of solutions. The structures of such systems substantially depend on the geometric factors (shape and sizes of the constituent particles), relative directions of the dipole moments and H bonds, *etc*. Apparently, the nonsphericity of particles enhances the collective character of their motion, thus assisting in strengthening the effects under consideration, which was observed in the studies of hydrazine systems[14,15,43] and N_2O_5 solutions in HNO_3.[48] Apparently, the existence of such thermodynamically stable diffusion-averaged solvation structures

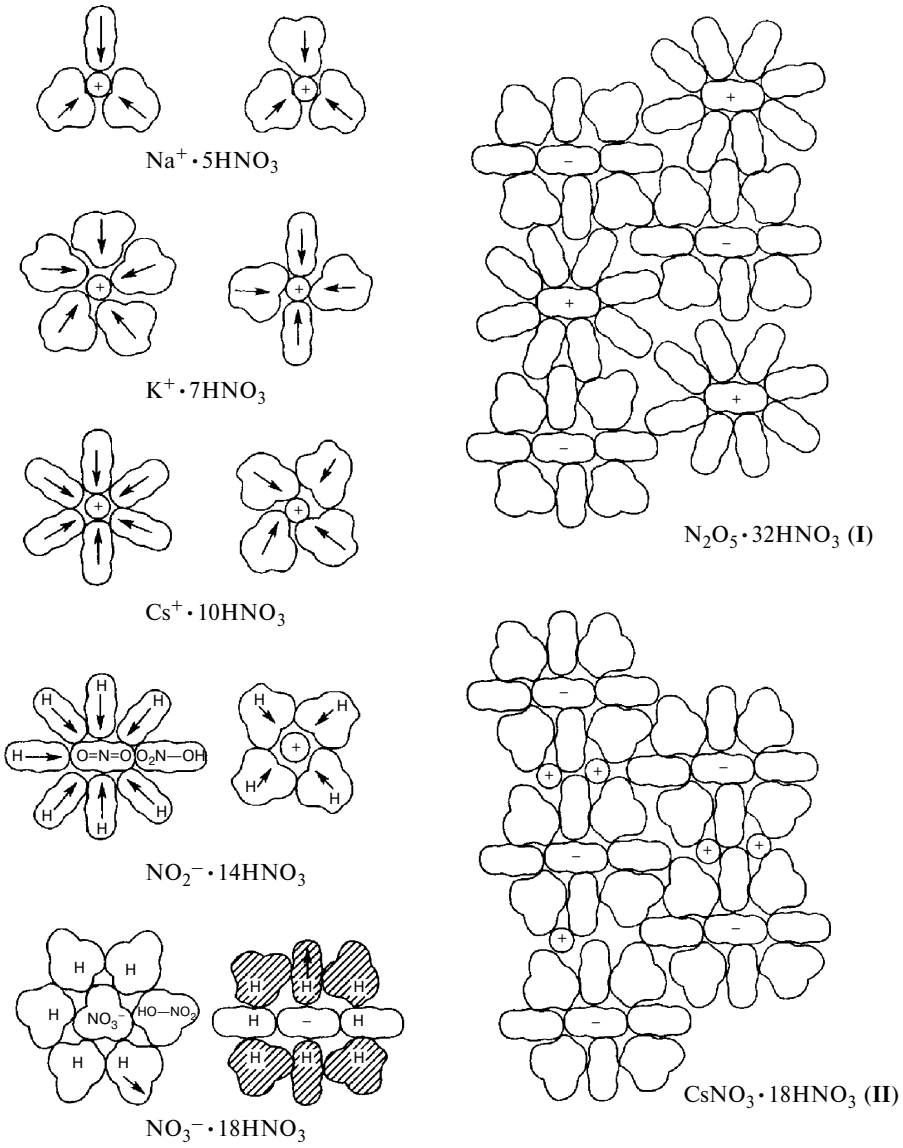

Fig. 18. Schematic representation of the solvation complexes of the M^+ cations and the NO_3^- anion in dilute MNO_3—HNO_3 solutions (views from two sides) and the solvation structures in concentrated solutions: the packing of the commensurate cation and anion solvation complexes in the structure of $N_2O_5 \cdot 32HNO_3$ (**I**), incorporation of the M^+ cation into the cavities between the solvation complexes of NO_3^- (**II**).

(unit cells of solutions) should be taken into account in the theoretical consideration and computer calculations of concentrated electrolyte solutions. In particular, calculations for compositions corresponding to special points, at which one solvation structure predominantly occurs, can be useful.

Interestingly, the related phenomena were observed in gaseous H-bonded ionic clusters. Studies of the size distribution of the clusters revealed the magic numbers, *i.e.*, the existence of relatively more stable compositions, and demonstrated that all these compositions correspond to structures with filled solvation shells.[42] In liquids, these effects can be strengthened due to interactions between solvation complexes.

Apparently, the observed effects are evidence in favor of the theory of liquids based on the hypothesis that simple one-component liquid systems have regions of local crystal ordering composed of ~10^2 particles.[77] This theory cannot be directly applied to the systems in question because of the two-component composition, nonsphericity of particles, and the presence of directed interactions. However, the first-order liquid—liquid phase transitions predicted by this theory would be expected to be observed in such complex systems.

4. Influence of supramolecular structures on the transformation of nonequilibrium anhydrous perchloric acid into equilibrium acid

Liquid anhydrous perchloric acid is an equilibrium system consisting of hydrogen perchlorate ($HOClO_3$) molecules, perchloric anhydride (Cl_2O_7) molecules, and H_3O^+ and ClO_4^- ions:

$$3\ HOClO_3 \rightleftharpoons Cl_2O_7 + H_3O^+ + ClO_4^-. \qquad (16)$$

The presence of small amounts of Cl_2O_7 and H_3OClO_4 in 100% perchloric acid has been documented for the first time in the study[78] and was than confirmed by numerous direct and indirect data.[60] Low equilibrium Cl_2O_7 and H_3OClO_4 concentrations strongly influence the thermal stability,[79] hydrating activity,[80] and other chemical and physical properties of perchloric acid. The equilibrium (16) is established not instantaneously.[81] If an $HClO_4$ vapor, which is obtained by heating a crystalline sample of H_3OClO_4 and contains no anhydride and monohydrate, is condensed at low temperature, the resulting nonequilibrium perchloric acid can be stored over a rather long period of time at temperatures below −30 °C. At −20 °C, the bands of Cl_2O_7 in the IR spectrum of the acid prepared as described above appear after 3.5 h; at 0 °C, after 15 min.

The wide use of nonequilibrium perchloric acid as the reagent and the medium for the synthesis of anhydrous perchlorates[80] necessitated precise data on the rate of the appearance of disproportionation products at different temperatures. The kinetics of disproportionation (16), *i.e.*, the transformation of nonequilibrium perchloric acid into equilibrium acid, was studied in the 10—25 °C temperature range by ^{1}H NMR spectroscopy.[53] The difficulty is that the transformation of the nonequilibrium acid into the equilibrium state is accompanied by changes in the chemical shifts in a very narrow range. Only the use of a NMR spectrometer with a strong magnetic field and the deuteration effect made it possible to perform direct kinetic measurements.

The procedure for the preparation of samples of nonequilibrium $HClO_4$ was developed in the study.[53]

4.1. Kinetics and mechanism of disproportionation of $HClO_4$. The study[54] of the dependence of the chemical shifts on the composition of aqueous solutions of perchloric acid (up to 100%) showed that, since the chemical shift of the monohydrate is similar to that of the acid (at 25 °C, these shifts are 5.800 and 5.520 ppm, respectively, relative to liquid water[54]), the sensitivity of ^{1}H NMR spectroscopy to the process under study is low. For example, an addition of 5% of the monohydrate to 100% $HClO_4$ leads to a change in the chemical shift by 0.014 ppm, *i.e.*, only by 4 Hz even at the operating frequency 294 MHz used in the spectrometer.[53] Experiments performed for two samples of $HClO_4$ demonstrated that the maximum difference in the observed chemical shifts of nonequilibrium and equilibrium perchloric acid measured under the same conditions is 3—4 Hz (Fig. 19). Since the small effect did not allow one to perform quantitative kinetic measurements for $HClO_4$, deuterated samples were used in further studies. For these samples, the sensitivity to the process under study is higher[54] (at 25 °C, the chemical shifts of the monohydrate and the acid in samples deuterated by 99% relative to liquid water are 7.074 and 5.591 ppm, respectively). Hence, the change in the chemical shift for the acid containing a 5% impurity of the monohydrate should be 22 Hz.

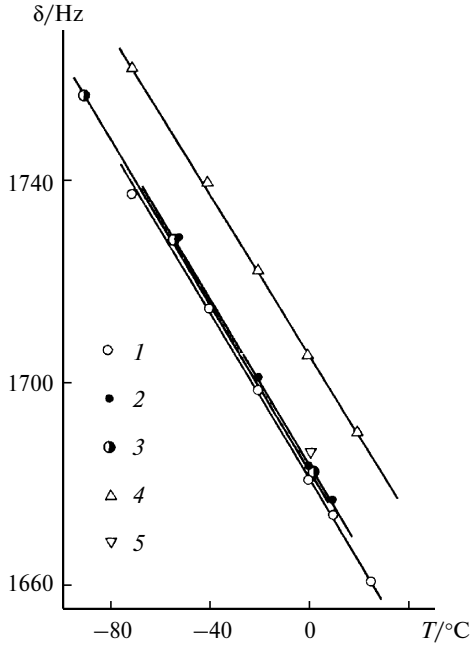

Fig. 19. Proton chemical shifts of equilibrium and nonequilibrium samples of perchloric acid *vs.* the temperature: *1* and *2*, nonequilibrium samples of $DClO_4$; *3*, a nonequilibrium sample of $HClO_4$; *4*, an equilibrium sample of $DClO_4$; *5*, an equilibrium sample of $HClO_4$.

Tests demonstrated that the expected strengthening of the effect actually occurred (see Fig. 19). The maximum differences in the chemical shifts of the residual protons in nonequilibrium and equilibrium samples are 20—25 Hz (observed chemical shift measured relative to the external standard varies within a few Hertzs due to the nonidentity of resonating cells). The strong influence of the isotopic H/D composition of the system on the proton chemical shifts is attributed to the fact that the isotope distribution between different states differs from the average distribution. The sign of this effect and direct experiments[82] demonstrated that the probability of the occurrence of the proton in the ionic forms in the

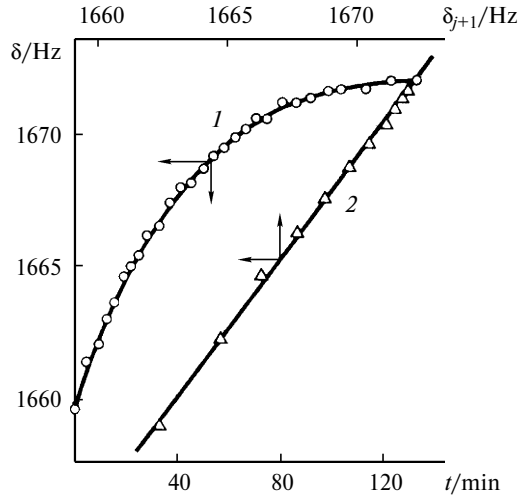

Fig. 20. Kinetic curve of the transformation of nonequilibrium perchloric acid into the equilibrium acid at 25 °C (*1*) and its linear anamorphose[83] (*2*).

states with strongest H bonds is higher compared to deuteron.*

The fact that the chemical shift of nonequilibrium perchloric acid in deuterated samples differs from that of the equilibrium acid by 20—25 Hz made it possible to measure the kinetic curves for four temperatures in high-precision experiments (this procedure has been described in detail in the study[43]). One kinetic curve (at 25 °C) along with its linear anamorphose[83] are presented in Fig. 20. A rather good linearization was observed in all cases, which indicates that the transformation is first order in a wide range of the degree of conversion (up to 70% of the total range). The temperature dependence of the transformation rate constant in the Arrhenius coordinates is presented in Fig. 21. The following activation energy E_a and the pre-exponential factor A_0 were obtained from this plot: $E_a = 77\pm4$ kJ mol^{-1} and $\log A_0 = 10.1\pm1.2$ with the probability of 0.9. It should be noted that in this case, the kinetic isotope effect is small, as is evident from a comparison with the results of experiments for samples with natural isotope abundance.

Based on the knowledge of the mechanism of thermal decomposition of perchloric acid and its aqueous solutions,[79] the following processes would be expected to occur:

$$HClO_4 + HClO_4 \underset{k_{-2}}{\overset{k_2}{\rightleftharpoons}} H_2ClO_4^+ + ClO_4^-, \qquad (17)$$

* Based on these concepts and the fact that the chemical shifts of nonequilibrium samples of deuterated perchloric acid are virtually identical to those of samples of this acid with natural isotope abundance, whereas the chemical shifts for equilibrium samples differ by 20—25 Hz, it can be concluded that an impurity of ionic states, which can form the strongest H bonds, is substantially smaller in the nonequilibrium acid compared to equilibrium samples.

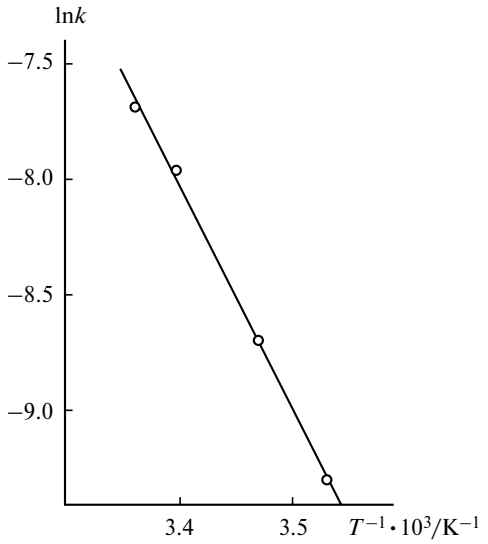

Fig. 21. Arrhenius plot for disproportionation of 100% perchloric acid.

$$H_2ClO_4^+ \underset{k_{-3}}{\overset{k_3}{\rightleftharpoons}} H_2O + ClO_3^+, \qquad (18)$$

$$H_2O + HClO_4 \underset{k_{-4}}{\overset{k_4}{\rightleftharpoons}} H_3O^+ + ClO_4^-, \qquad (19)$$

$$ClO_4^- + ClO_3^+ \underset{k_{-5}}{\overset{k_5}{\rightleftharpoons}} Cl_2O_7. \qquad (20)$$

Among these processes, the reaction (18) is the slowest one. In this case,

$$d[H_3O^+]/dt = k_3[H_2ClO_4^+] - k_{-3}[H_2O][ClO^{3+}].$$

Since

$$K_2 = \frac{[ClO_4^-][H_2ClO_4^+]}{[HClO_4]^2},$$

$$K_4 = \frac{[H_3O^+][ClO_4^-]}{[H_2O][HClO_4]},$$

$$\frac{d[H_3O^+]}{dt} = k_3\frac{K_2[HClO_4]^2}{[ClO_4^-]} - k_{-3}\frac{[H_3O^+][ClO_3^+][ClO_4^-]}{K_4[HClO_4]},$$

then

$$d\eta/dt = k^{(1)}\eta^{-1} - k^{(2)}\eta^2,$$

where η is the degree of conversion equal to $[H_3O^+]/[HClO_4]_0$, taking into account $[H_3O^+] \approx [ClO_4^-] \approx [C1_2O_7]$ and $[HClO_4]_0 \approx [HClO_4]$. Based on the change in the chemical shift, the equilibrium degree of conversion $\eta_0 = 0.05$—0.07, which gives the constant ratio $k^{(1)}/k^{(2)} = 10^{-4}$. Tests demonstrated that the linear dependence of $d\eta/dt$ on η typical of the first-order processes can be observed only in a rather narrow range of

the degrees of conversion (≤20% of the equilibrium η_0) as opposed to the real situation.

Therefore, the above-considered scheme does not account for the observed features. However, the experimentally observed first order can be explained with the use of the concepts (see the above sections) of the formation of labile supramolecular structures in this type of systems. At the initial instant of time, pure nonequilibrium perchloric acid exists as a weakly ionized but (based on the chemical shifts and vibrational spectra[81]) rather strongly H-bonded liquid. Self-associates of this acid can be represented, for example, as cyclic dimers, the equilibrium

$$2\,HClO_4 \underset{}{\overset{K_6}{\rightleftharpoons}} (HClO_4)_2 \qquad (21)$$

being shifted to the right.

Let us assume that the following reaction is the rate-limiting step of disproportionation

$$(HClO_4)_2 \underset{k_{-7}}{\overset{k_7}{\rightleftharpoons}} H_2O + Cl_2O_7. \qquad (22)$$

The resulting H_2O molecules rapidly react with $HClO_4$ to form H_3O^+ and ClO_4^- ions, thus decreasing the number of acid molecules by including them in solvation shells:

$$H_2O + (m + n + 1)\,HClO_4 \overset{K_{4a}}{\rightleftharpoons} \rightleftharpoons (H_3O^+)\cdot m HClO_4 + (ClO_4^-)\cdot n HClO_4. \qquad (19a)$$

As a result, the concentration of dimers sharply decreases and the process is terminated.

Analysis of the equation system describing the transformations (19a), (21), and (22) leads to the following kinetic law

$$\frac{d\eta}{dt} = \frac{k_7}{2}[1 - (m + n + 3)\eta] - \frac{k_{-7}\eta^3 (2K_6)^{(m+n+1)/2}}{K_{4a}[1 - (m + n + 3)\eta]^{(m+n+1)/2}}.$$

When the second term corresponding to the reverse reaction is small and plays a certain role only in the very end of the process, disproportionation occurs according to the first-order kinetics. Taking into account the ratio $\eta_0 \approx 1/(m + n + 3)$ and assuming that the equilibrium degree of conversion $\eta_0 = 0.06 \pm 0.01$, we obtain the number of molecules in the solvation shells $m + n = 14 \pm 3$, which is quite reasonable for this type of systems.[14,43] From this scheme it also follows that the decrease in the acid concentration to $1 - \eta_0$, *i.e.*, to ~95 mol.%, will lead to a sharp decrease in the equilibrium concentrations of perchloric anhydride, which agrees with the data on thermal decomposition[79] and vapor pressures[60] for these systems.

5. Conclusion

The review demonstrates that structuration of associated pure liquids and electrolyte solutions in these liquids can be be studied experimentally by NMR spectroscopy. Examples of the influence of this structural self-organization on the chemical kinetics and thermodynamics are given. The following advantages of NMR spectroscopy are noted:

— possibility of obtaining quantitative data on directed interactions, primarily, in H-bonded systems;

— possibility of determining fine specific features of the concentration and temperature dependences, which bear information on the structural self-organization in liquids;

— high accuracy of quantitative measurements of the kinetics of fast chemical exchanges, in which the role of self-organization is most pronounced.

This made it possible to obtain data not only on the compositions and structures of labile supramolecular systems but also on the dynamics of their reorganization in the liquids under study.

These studies provided a deeper insight into the mechanism of the fundamental process of "structural diffusion" (proton mobility in liquids as diffusion of an H^+-induced structural defect in the H-bond network of the liquid) and gave estimates of the dependence of this process on solvophobic substituents and structural motifs of supramolecular systems involved in reorganization.

A thorough study of a number of systems led us to conclude that there are special points in liquids, *i.e.*, the magic relations between the mole concentrations and the "critical" temperatures in the close vicinity of which the derivatives of the physicochemical properties (and sometimes, the properties by themselves) change much more sharply than in the adjacent regions. In our opinion, thermodynamically stable diffusion-averaged supramolecular structures correspond to these singular points. In the case of compositions intermediate between two special points, the system is a quasi-ideal mixture consisting predominantly of two structures, which correspond to the adjacent special points and exist in the dynamic equilibrium. Our experience in studying various inorganic and organic systems demonstrated that these effects are widespread (these effects are known, for example, for aqueous-alcoholic systems) and can be accompanied by considerable thermodynamic and kinetic effects.

Long-lived structures, which are based on H bonds and other intermolecular forces, contain a large number of particles, and are characterized by a complex architecture, have been extensively studied in past decades in supramolecular chemistry and hold great promise.[84—86] Solvation complexes and associates in the liquid phase are essentially labile supramolecular systems. However, in spite of a considerable progress in this field,[87,88] these systems are poorly studied. This is associated with the fact that experimental studies of such systems present difficulties because of the averaging due to particle motion in liquids. In addition, there are no adequate theories of the

liquid state because it is difficult to take into account collective interactions.

References

1. M. Tuckerman, K. Laasonen, M. Sprik, and M. Parrinello, *J. Phys. Chem.*, 1995, **99**, 5749; M. Tuckerman, K. Laasonen, M. Sprik, and M. Parrinello, *J. Chem. Phys.*, 1995, **103**, 150.
2. N. Agmon, *Chem. Phys. Lett.*, 1995, **244**, 456.
3. N. Agmon, *J. Chim. Phys.*, 1996, **93**, 1714.
4. M. Pavese, S. Chawla, D. S. Lu, J. Lobaugh, and G. A. Voth, *J. Chem. Phys.*, 1997, **107**, 7428.
5. R. Vuilleumier and D. Borgis, *J. Mol. Struct.*, 1997, **437**, 555; R. Vuilleumier and D. Borgis, 1998, *Chem. Phys. Lett.*, **284**, 71.
6. M. Pavese and G. A. Voth, *Ber. Bunsen. Phys. Chem.*, 1998, **102**, 527.
7. N. Agmon, *Israel J. Chem.*, 1999, **39**, 493.
8. D. Marx, M. E. Tuckerman, J. Hutter, and M. Parrinello, *Nature*, 1999, **397**, 601.
9. J. T. Hynes, *Nature*, 1999, **397**, 565.
10. K. D. Kreuer, *Chem. Mater.*, 1996, **8**, 610; A. B. Yaroslavtsev and V. Yu. Kotov, *Izv. Akad. Nauk, Ser. Khim.*, 2002, 515 [*Russ. Chem. Bull., Int. Ed.*, 2002, **51**, 555].
11. N. G. Yunda, G. V. Lagodzinskaya, and G. B. Manelis, *Izv. Akad. Nauk SSSR, Ser. Khim.*, 1975, 2443 [*Bull. Acad. Sci. USSR, Div. Chem. Sci.*, 1975, **24**, 2330 (Engl. Transl.)].
12. N. G. Yunda, G. V. Lagodzinskaya, E. B. Fel´dman, and G. B. Manelis, *Izv. Akad. Nauk SSSR, Ser. Khim.*, 1977, 1285 [*Bull. Acad. Sci. USSR, Div. Chem. Sci.*, 1977, **26**, 1181 (Engl. Transl.)].
13. G. V. Lagodzinskaya, N. G. Yunda, and G. B. Manelis, *Izv. Akad. Nauk SSSR, Ser. Khim.*, 1980, 778 [*Bull. Acad. Sci. USSR, Div. Chem. Sci.*, 1980, **29**, 532 (Engl. Transl.)].
14. G. V. Lagodzinskaya, N. G. Yunda, and G. B. Manelis, *Izv. Akad. Nauk SSSR, Ser. Khim.*, 1980, 987 [*Bull. Acad. Sci. USSR, Div. Chem. Sci.*, 1980, **29**, 695 (Engl. Transl.)].
15. G. V. Lagodzinskaya, N. G. Yunda, and G. B. Manelis, *Izv. Akad. Nauk SSSR, Ser. Khim.*, 1981, 953 [*Bull. Acad. Sci. USSR, Div. Chem. Sci.*, 1981, **30**, 724 (Engl. Transl.)].
16. N. G. Yunda, G. V. Lagodzinskaya, and G. B. Manelis, *Izv. Akad. Nauk SSSR, Ser. Khim.*, 1972, 1284 [*Bull. Acad. Sci. USSR, Div. Chem. Sci.*, 1972, **21** (Engl. Transl.)].
17. N. G. Yunda, Ph. D. (Chem.) Thesis, Institute of Problems of Chemical Physics, Russian Academy of Sciences, Chernogolovka, 1992 143 pp. (in Russian).
18. G. V. Lagodzinskaya, N. G. Yunda, and G. B. Manelis, *Chem. Phys.*, 2002, **282**, 51.
19. G. Zundel and J. Fritsch, in *The Chemical Physics of Solvation*, Eds R. R. Dogonadze, E. Kalman, A. A. Kornyshev, and J. Ulstrup, Elsevier, Amsterdam, 1986, **2**, 21.
20. B. Brzezinski and G. Zundel, *J. Chem. Soc., Faraday Trans. 2*, 1979, **75**, 661.
21. H.-P. Cheng, *Phys. Chem. A*, 1998, **102**, 6201.
22. D. R. Clutter and T. J. Swift, *J. Am. Chem. Soc.*, 1968, **90**, 601.
23. P. W. Atkins, A. Loewenstein, and Y. Margalit, *Mol. Phys.*, 1969, **17**, 329.
24. J. D. Halliday, P. E. Binder, and S. Padamshi, *Can. J. Chem.*, 1984, **62**, 1258.
25. F. Huisken and T. Pertsch, *Chem. Phys.*, 1988, **126**, 213.
26. D. Gerritzen and H. H. Limbach, *Ber. Bunsen-Ges. Phys. Chem.*, 1981, **85**, 527.
27. V. A. Daragan, A. U. Stepanyants, and T. N. Khazanovich, *Zh. Strukt. Khim.,* 1978, **19**, 474 [*J. Struct. Chem. USSR*, 1978, **19** (Engl. Transl.)].
28. W. A. P. Luck, *Acta Chim. Hung.*, 1986, **121**, 119.
29. H. G. Hertz, in *Progress in Nuclear Magnetic Resonance Spectroscopy*, Eds J. W. Emsley, F. Feeney, and L. H. Sutcliffe, Pergamon Press, Oxford—London, 1967, **3**, 159.
30. A. Loewenstein and A. Szoke, *J. Am. Chem. Soc.*, 1962, **84**, 1151.
31. L. Pauling, *The Nature of Hydrogen Bond*, Oxford University Press, Ithaca—New York, 1960.
32. W. L. Jorgensen, *J. Am. Chem. Soc.*, 1980, **102**, 543.
33. S. Sarkar, A. K. Karmakar, and R. N. Joarder, *J. Phys. Chem. A*, 1997, **101**, 3702.
34. Y. Kamishina, *J. Magn. Res.*, 1975, **20**, 388.
35. R. L. Collin and W. N. Lipscomb, *Acta Crystallogr.*, 1951, **4**, 10.
36. B. G. Rao and U. C. Singh, *J. Am. Chem. Soc.*, 1991, **113**, 4381.
37. J. Pople, W. Schneider, and H. Bernstein, *High-Resolution Nuclear Magnetic Resonance*, McGraw-Hill, New York, 1959.
38. M. Saunders and J. Hune, *J. Chem. Phys.*, 1958, **29**, 1319.
39. J. C. Hindman, *J. Chem. Phys.*, 1966, **44**, 4582.
40. S. E. Odinokov, A. A. Mashkovskii, and A. K. Dzizenko, *Dokl. Akad. Nauk SSSR,* 1975, **220**, 1130 [*Dokl. Chem.*, 1975 (Engl. Transl.)].
41. H. C. Chang, J. C. Jiang, S. H. Lin, Y. T. Lee, and H. C. Chang, *J. Phys. Chem. A*, 1999, **103**, 2941.
42. M. T. Coolbaugh and J. F. Garvey, *Chem. Soc. Rev.*, 1992, 163.
43. G. V. Lagodzinskaya, I. Yu. Kozyreva, N. G. Yunda, and G. B. Manelis, *Izv. Akad. Nauk SSSR, Ser. Khim.*, 1984, 2212 [*Bull. Acad. Sci. USSR, Div. Chem. Sci.*, 1984, **33**, 2017 (Engl. Transl.)].
44. N. M. Emanuel´ and D. G. Knorre, *Kurs khimicheskoi kinetiki* [*Handbook of Chemical Kinetics*], Vysshaya shkola, Moscow, 1969, 432 pp. (in Russian).
45. V. I. Chizhik, Dr. Sc. (Chem.) Thesis, Leningrad State University, Leningrad, 1981, 46 pp. (in Russian).
46. P. A. Zagorets, V. I. Ermakov, and A. P. Grunau, *Zh. Fiz. Khim.*, 1965, **39**, 9 [*J. Phys. Chem. USSR*, 1965, **39** (Engl. Transl.)].
47. Yu. S. Bogachev and N. N. Shapet´ko, *Zh. Fiz. Khim.*, 1988, **62**, 2617 [*J. Phys. Chem. USSR*, 1988, **62** (Engl. Transl.)].
48. G. V. Lagodzinskaya, N. G. Yunda, E. P. Kirpichev, A. I. Kazakov, Yu. I. Rubtsov, V. O. Zavel´skii, and G. B. Manelis, *Khim. Fiz.*, 1989, 236 [*Chem. Phys. USSR*, 1989 (Engl. Transl.)].
49. G. V. Lagodzinskaya, M. V. Loginova, N. G. Yunda, V. O. Zavel´skii, and G. B. Manelis, *Koord. Khim.,* 1998, **24**, 152 [*Russ. J. Coord. Chem.*, 1998, **24** (Engl. Transl.)].
50. V. I. Ermakov, V. V. Shcherbakov, and S. B. Khubetsov, *Zh. Fiz. Khim.*, 1973, **47**, 728 [*J. Phys. Chem. USSR*, 1973, **47** (Engl. Transl.)].
51. J. Burgess, *Ions in Solution: Basic Principles of Chemical Interaction*, Halsted Press, Chichester, 1988.
52. H. Ohtaki and T. Radnai, *Chem. Rev.*, 1993, **93**, 1157.

53. G. V. Lagodzinskaya, G. B. Manelis, Z. K. Nikitina, V. I. Shestov, and V. Ya. Rosolovskii, *Izv. Akad. Nauk SSSR, Ser. Khim.*, 1985, 781 [*Bull. Acad. Sci. USSR, Div. Chem. Sci.*, 1985, **34**, 708 (Engl. Transl.)].
54. R. W. J. Duerst, *Chem. Phys.*, 1968, **48**, 2275.
55. Yu. V. Karyakin and N. N. Angelov, *Chistye khimicheskie veshchestva* [*Pure Chemical Substances*], Khimiya, Moscow, 1974, 407 pp. (in Russian).
56. F. Daniels and F. Bright, *J. Am. Chem. Soc.*, 1921, **43**, 53.
57. K. V. Titova, E. P. Kirpichev, and V. Ya. Rosolovskii, *Tez. dokl., IX Vsesoyuzn. konf. "Kalorimetriya i khimicheskaya termodinamika"* [*Abstrs. of Papers, IX All-Union Conf. "Calorimetry and Chemical Thermodynamics"*], Tbilisi, 1982, 20 (in Russian).
58. I. Yu. Kozyreva, G. V. Lagodzinskaya, Z. B. Maiofis, and E. B. Fel´dman, *Teoret. Eksp. Khim.*, 1984, **20**, 452 [*Theor. Exp. Chem.*, 1084, **20** (Engl. Transl.)].
59. G. V. Lagodzinskaya and I. Yu. Klimenko, *J. Magn. Res.*, 1982, **49**, 1.
60. V. Ya. Rosolovskii, *Khimiya bezvodnoi khlornoi kisloty* [*Chemistry of Anhydrous Perchloric Acid*], Nauka, Moscow, 1966, 140 pp. (in Russian).
61. O. Ya. Samoilov, *Sostoyanie i rol´´ vody v biologicheskikh ob"ektakh* [*State and Role of Water in Biological Materials*], Nauka, Moscow, 1967, 31 pp. (in Russian).
62. N. B. Librovich, V. P. Sakun, and N. D. Sokolov, in *Vodorodnaya svyaz* [*Hydrogen Bond*], Nauka, Moscow, 1981, 174 pp. (in Russian).
63. D. Eizenberg and V. Kautsman, *Struktura i svoistva vody* [*Structure and Properties of Water*], Gidrometeoizdat, Leningrad, 1975, 280 pp. (in Russian).
64. C. C. Addison, *Chem. Rev.*, 1980, **80**, 21.
65. S. S. Odokienko, N. V. Latypov, I. N. Shokhor, Yu. A. Fedorov, and E. N. Vishnevskii, *Zh. Prikl. Khim.*, 1978, **51**, 683 [*J. Appl. Chem. USSR*, 1978, **51** (Engl. Transl.)].
66. C. C. Addison and N. Logan, in *Developments in Inorganic Nitrogen Chemie*, Ed. C. B. Colburn, Elsevier, Amsterdam, 1973, **2**, 27. z
67. B. V. Nekrasov, *Osnovy obshchei khimii* [*Fundamentals of General Chemistry*], Khimiya, Moscow, 1973, **1**, 428 pp. (in Russian).
68. E. Berl and H. H. Saenger, *Monatsh. Chem.*, 1929, **54**, 1036.
69. A. G. Udovenko, V. A. Granzhan, and D. N. Bugun, *Vyazkost´ i poverkhnostnoe natyazhenie rastvorov v N_2O_4 i N_2O_5 azotnoi kislote* [*Viscosity and Surface Tension of N_2O_4 and N_2O_5 Solutions in Nitric Acid*], Leningrad, 1983, 5 pp.; Deposited in VINITI, 29.03.83, No. 1553-83 (in Russian).
70. G. M. Kurbatov and I. I. Skorokhodov, *Zh. Neorg. Khim.*, 1976, **21**, 2576 [*J. Inorg. Chem. USSR*, 1976, **21** (Engl. Transl.)].
71. G. M. Shutov, O. G. Ul´ko, L. M. Efremova, and E. Yu. Orlova, *Kinetika i mekhanizm termicheskogo razlozheniya rastvorov N_2O_5 v azotnoi kislote i rastvorov HNO_3 v sernoi kislote* [*Kinetics and Mechanism of Thermal Decomposition of N_2O_5 Solutions in Nitric Acid and of HNO_3 Solutions in Sulfuric Acid*], Moscow, 1982, 7 pp.; Deposited in VINITI 07.04.82, No. 2350-82 (in Russian).
72. O. P. Yablonskii, *Zh. Fiz. Khim.*, 1975, **49**, 2538 [*J. Phys. Chem. USSR*, 1975, **49** (Engl. Transl.)].
73. J.-P. Kintzinger, in *Nuclear Magnetic Resonance. Basic Principles and Progress*, Eds P. Diehl, E. Fluck, and R. Kosfield, Springer, Berlin, 1981, **17**, 1.
74. M. A. Anisimov, *Kriticheskie yavleniya v zhidkostyakh i zhidkikh kristallakh* [*Critical Phenomena in Liquids and Liquid Crystals*], Nauka, Moscow, 1987 (in Russian).
75. K. P. Mishchenko and G. M. Poltoratskii, *Voprosy termodinamiki i stroeniya vodnykh i nevodnykh rastvorov elektrolitov* [*Problems of Thermodynamics and Structures of Aqueous and Nonaqueous Electrolyte Solutions*], Khimiya, Leningrad, 1968, 352 pp. (in Russian).
76. G. Zundel, in *Trends in Physical Chemistry*, Ed. J. Menon, Research Trends, Trivandrum, 1992, **2**, 129.
77. A. C. Mitus and A. Z. Patashinskii, *Phys. Lett.*, 1985, **113A**, 41.
78. H. J. Van Wyk, *Z. anorg. und allg. Chem., B*, 1906, **48**, 1.
79. Yu. I. Rubtsov, G. B. Manelis, Z. I. Grigorovich, and V. Ya. Rosolovskii, *Zh. Fiz. Khim.*, 1974, **48**, 1399 [*J. Phys. Chem. USSR*, 1974, **48** (Engl. Transl.)].
80. Z. K. Nikitina and V. Ya. Rosolovskii, *Izv. Akad. Nauk SSSR, Ser. Khim.*, 1977, 1466 [*Bull. Acad. Sci. USSR, Div. Chem. Sci.*, 1977, **26** (Engl. Transl.)].
81. A. I. Karelin, Z. I. Grigorovich, and V. Ya. Rosolovskii, *Izv. Akad. Nauk SSSR, Ser. Khim.*, 1975, 665 [*Bull. Acad. Sci. USSR, Div. Chem. Sci.*, 1975, **24** (Engl. Transl.)].
82. N. S. Golubev, *Khim. Fiz.*, 1983, 42 [*Chem. Phys. USSR*, 1983 (Engl. Transl.)].
83. E. S. Swinbourne, *J. Chem. Soc.*, 1960, 2371.
84. J.-M. Lehn, *Concepts and Perspectives: A Personal Account*, Wiley VCH, Paperback, 1995.
85. J.-M. Lehn, *Proc. Natl. Acad. Sci. USA*, 2002, **99**, 4763.
86. J.-M. Lehn, *J. Coord. Chem.*, 1992, **27**, 3.
87. V. A. Durov, *J. Mol. Liquids*, 2005, **118**, 101.
88. M. G. Kiselev, Dr. Sc. (Chem.) Thesis, Institute of Solution Chemistry of the Russian Academy of Sciences, Ivanovo, 2003, 292 pp. (in Russian).

Received December 13, 2005;
in revised form April 29, 2006